CIVIL ENGINEERING STUDIES
Illinois Center for Transportation Series No. 20-022
UILU-ENG-2020-2022
ISSN: 0197-9191

Bridge Decks: Mitigation of Cracking and Increased Durability—Phase III

Prepared By
Mohammad Rahman
Ahmed Ibrahim
Riyadh Hindi
Saint Louis University

Research Report No. FHWA-ICT-20-015

A report of the findings of

ICT PROJECT R27-178-2
Bridge Decks: Mitigation of Shrinkage Cracking—Phase III

https://doi.org/10.36501/0197-9191/20-022

Illinois Center for Transportation

December 2020

TECHNICAL REPORT DOCUMENTATION PAGE

1. Report No.	2. Government Accession No.	3. Recipient's Catalog No.
FHWA-ICT-20-015	N/A	N/A

4. Title and Subtitle	5. Report Date
Bridge Decks: Mitigation of Cracking and Increased Durability—Phase III	December 2020
	6. Performing Organization Code N/A

7. Authors	8. Performing Organization Report No.
Mohammad Rahman, Ahmed Ibrahim, and Riyadh Hindi	ICT-20-022 UILU-2020-2022

9. Performing Organization Name and Address	10. Work Unit No.
Illinois Center for Transportation Department of Civil and Environmental Engineering University of Illinois at Urbana-Champaign 205 North Mathews Avenue, MC-250 Urbana, IL 61801	N/A
	11. Contract or Grant No. R27-178-2

12. Sponsoring Agency Name and Address	13. Type of Report and Period Covered
Illinois Department of Transportation (SPR) Bureau of Research 126 East Ash Street Springfield, IL 62704	Final Report 9/15/17–12/15/20
	14. Sponsoring Agency Code

15. Supplementary Notes

Conducted in cooperation with the U.S. Department of Transportation, Federal Highway Administration.
https://doi.org/10.36501/0197-9191/20-022

16. Abstract

Early-age cracking in concrete decks significantly reduces the service life of bridges. This report discusses the application of various concrete mixtures that include potential early mitigation ingredients. Large-scale (7 ft × 10 ft) experimental bridge prototypes with similar restraint conditions found in actual bridges were poured with different concrete mixtures to investigate mitigation techniques. Portland cement (control), expansive Type K cement, internally cured lightweight aggregate (LWA), shrinkage-reducing admixture (SRA), and gypsum mineral were investigated as mitigating ingredients. Seven concrete mixtures were prepared by using individual ingredients as well as a combination of different ingredients. The idea behind combining different mitigating techniques was to accumulate the combined benefit from individual mitigating materials. The combined Type K cement and LWA mixture showed higher concrete expansion compared with mixtures containing Portland cement, Type K cement, LWA, and SRA in the large-scale experimental deck. Extra water provided by LWA significantly enhanced the performance of Type K cement's initial expansion as well as caused larger total shrinkage over the drying period. A combination of Type K cement and gypsum mineral showed insignificantly higher expansion compared with the individual Type K mixture. Overall, the experimental deck containing SRA showed the least total shrinkage compared with other mixtures. Finite-element modeling was performed to evaluate and predict concrete stress-strain behavior due to shrinkage in typical bridges. A parametric study using finite-element analysis was conducted by altering the structure of the experimental deck. More restraint from internal reinforcement, less girder spacing, larger girder flange width, and more restrictive support conditions increased the concrete tensile stress and led to potential cracking in the concrete deck.

17. Key Words	18. Distribution Statement
Concrete Shrinkage, Bridge Decks, Cracking and Durability	No restrictions. This document is available through the National Technical Information Service, Springfield, VA 22161.

19. Security Classif. (of this report)	20. Security Classif. (of this page)	21. No. of Pages	22. Price
Unclassified	Unclassified	48 + appendix	N/A

Form DOT F 1700.7 (8-72) **Reproduction of completed page authorized**

ACKNOWLEDGMENT, DISCLAIMER, MANUFACTURERS' NAMES

This publication is based on the results of **ICT-R27-178-2: Bridge Decks: Mitigation of Cracking and Increased Durability—Phase III**. ICT-R27-178-2 was conducted in cooperation with the Illinois Center for Transportation; the Illinois Department of Transportation; and the U.S. Department of Transportation, Federal Highway Administration.

Members of the Technical Review Panel (TRP) were the following:

- James Krstulovich, Illinois Department of Transportation
- Hani Alnamer, Illinois Department of Transportation
- Julie Beran, Illinois Department of Transportation
- Mike Copp, Illinois Department of Transportation
- Darrin Davis, Illinois Department of Transportation
- Kevin Reichers, Illinois Department of Transportation
- Dan Tobias, Illinois Department of Transportation
- Melinda Winkelman, Illinois Department of Transportation
- Steve Worsfold, Illinois Department of Transportation
- Dan Brydl, Federal Highway Administration
- Randy Riley, formerly Illinois Chapter, American Concrete Pavement Association

EXECUTIVE SUMMARY

Early-age cracking in concrete bridge decks is one of the major concerns for bridge owners and state departments of transportation. Crack prevention is a challenging problem, and various studies have reported alternatives that try to eliminate or reduce bridge deck cracking. Concrete deck cracks significantly reduce the service life of bridges and lead to quick deterioration because cracks maximize chloride diffusion during wintertime and consequently produce reinforcement corrosion. This study investigates the implementation of different mitigation techniques to potentially reduce early-age shrinkage cracking in bridge decks.

Large-scale experimental bridge prototypes have been built and tested concurrently to investigate various types of concrete mixtures that include potential early mitigation ingredients. The implementation of concrete mixtures in the large-scale bridge prototype was based on the results of fresh and mechanical concrete properties tests, which are hereafter defined as small-scale experiments. There is a major variance between the structural behavior of small-scale testing and the actual bridge deck because of the differences in boundary conditions and the intensity of restraint levels provided by coarse aggregate and steel reinforcement. Steel girders, shear studs, reinforcing bars, and aggregates provide restraint against concrete volume change in bridge decks. Restrained shrinkage produces internal residual tensile stress in concrete structures and eventually causes cracking. The experimental deck introduced in this study was built to mimic similar restraint conditions found in actual Illinois Department of Transportation (IDOT) bridge decks.

Two large-scale bridge decks were tested in Phase I of this research project, including a typical control mixture used by IDOT in Illinois bridges and a mixture containing Type K expansive cement. Type K cement had a higher early-age expansion compared with the control mixture but showed a similar shrinkage rate during the six-month drying period.

Two additional mixtures were investigated in Phase II of the research project, including lightweight aggregate (LWA) and shrinkage-reducing admixture (SRA). The results showed that SRA had the least total shrinkage at the end of the drying period and LWA had a lower shrinkage rate compared to all mixtures.

In the current phase of the research project (Phase III), three additional large-scale bridge decks were monitored using a combination of previous mitigating mixtures. The main idea behind combining different mitigating techniques was to accumulate the combined benefit from individual mitigating materials. Experimental decks were poured with three different mixtures known as Type K+LWA (I), Type K+LWA (II), and Type K+Gypsum. The results from the Type K+Gypsum mixture did not show any notable expansion when compared with the individual Type K mixture. The Type K+Gypsum mixture showed slightly increased shrinkage (6%) at the end of the drying period compared with the control deck.

In contrast, the Type K+LWA mixtures showed considerably higher expansion at early ages. The Type K+LWA (I) and Type K+LWA (II) mixtures had approximately 104% and 62% higher expansion compared with the individual Type K mixture, respectively. At the end of the drying period, Type

K+LWA (I) and Type K+LWA (II) mixtures showed 19% and 33% less shrinkage compared with the individual Type K mixture, respectively. Internal curing from LWA promoted higher expansion during the hydration period with the existence of Type K cement.

In addition to the experimental work, analytical investigation through finite-element modeling was conducted to evaluate the shrinkage-induced strain within a bridge deck. Finite-element simulation was used to predict the shrinkage of concrete decks with reasonable accuracy. The results also showed that a higher amount of restraint inside the deck produces higher tensile stress within the deck.

TABLE OF CONTENTS

LIST OF FIGURES

LIST OF TABLES

CHAPTER 1: INTRODUCTION

Extensive research has been performed on bridge deck performance using small-scale specimens. However, major differences exist between a bridge deck's actual performance and small-scale specimen tests, including the boundary and intensity of restraint condition. The experimental deck introduced in this study has a restraint condition similar to actual bridge decks. Large-scale experimental bridge decks of 7 ft x 10 ft were constructed with different shrinkage-mitigating mixtures.

Type K cement is an expansive cementitious material that compensates for drying shrinkage through early-age expansion during the hydration period (Chaunsali et al., 2013; Nagataki & Gomi, 1998; Pittman et al., 1999; Rahman et al., 2018; Richardson et al., 2014). The early-age expansion mechanism of Type K cement forms stable ettringite crystals. Proper moist curing is important for the formation and expansion of ettringite crystals. Internally cured lightweight aggregate slowly releases the absorbed water and slows the rate of shrinkage in the concrete deck (Bentz & Weiss, 2011; Rahman et al., 2019). Combining internally cured lightweight aggregate with Type K expansive cement could be a technique to accumulate the benefits in mitigating drying shrinkage. Previous research showed that the addition of gypsum—hydrated calcium sulfate in a chemical form—with fly ash increases the compressive strength and durability of stabilized fly ashes (Aimin & Sarkar, 1991). The addition of gypsum in concrete mixtures significantly regulates the setting time of cement and mitigates the consumption of ye'elimite by class C fly ash. Those types of mixtures have been used in in many departments of transportation. The addition of gypsum in the Type K mixture could possibly enhance early-age expansion by delaying the setting time of concrete.

Previous studies have examined optimizing the structural design of bridge superstructures, including changing the number of shear studs or the spacing between reinforcement (French et al., 1999; Frosch et al., 2002; Schmitt & Darwin, 1995). Some studies have also found that lowering the amount of restraint inside the concrete deck could help reduce crack formation as well. Nagataki and Gomi (1998) modeled bridge deck shrinkage and found that reinforcement within the deck leads to high tensile stresses in the concrete deck. Frosch et al. (2002) also showed that the reinforcement ratio could change the number of cracks in concrete bridge decks. In addition, a parametric study using computer modeling also showed that cracks formed due to the differential shrinkage between the concrete bridge deck and girders (Tej et al., 2014).

CHAPTER 2: BRIDGE DECK EXPERIMENTAL TESTING

This chapter presents the set up and testing procedures of large-scale experimental bridge decks. The scaled bridge deck was built at the material and structural testing laboratory at Saint Louis University. The concrete mixtures used in this study were designed with various ingredient combinations of lightweight aggregate (LWA), Type K cement, gypsum, and shrinkage-reducing admixtures (SRA). The goal of this study is to compare the results of the small-scale laboratory experiments to the large-scale bridge prototype to understand the structural effects of a full-scale bridge on shrinkage behavior, concrete cracking mechanisms, and durability.

Four bridge decks were tested using four different concrete mixtures in Phases I and II of this research project. In Phase I, the typical control mixture and expansive Type K cement mixtures were tested using experimental bridge bays. The results showed that the Type K mixture had higher expansion at an early age compared to the control concrete mixture (Chaunsali et al., 2013). In Phase II, two other mixtures using LWA and SRA were tested using the large-scale bridge bays. The results showed that the LWA mixture had a flatter shrinkage strain slope compared to other mixtures and SRA showed a minimal shrinkage strain when compared to other mixtures (Ardeshirilajimi et al., 2016).

Three additional bridge decks were tested using newly developed concrete mixtures in the current phase of this research project (Phase III). Two of the bridge bays were poured with a combination of Type K and LWA (Type K+LWA) with various concrete mixture ingredients. Another bridge deck was monitored with a concrete mixture made from a combination of Type K and gypsum mineral (Type K+Gypsum). The results from the Phase III experimental decks are compared and discussed in this chapter.

BRIDGE BAY DESIGN

Experimental bridge decks were designed following the guidelines provided by the Illinois Department of Transportation (IDOT) standard concrete deck design. The deck was 7 ft × 10 ft (2 m × 3 m) with a typical thickness of 8 in. (20 cm), which was selected based on IDOT's standard *Bridge Design Manual* (2012), as shown in Figures 1 and 2. Two layers of #5 epoxy-coated reinforcing bars were placed longitudinally and transversely. Two W12×79 steel girders were spaced at 5 ft (1.5 m) to support the experimental bridge deck. Shear studs were spaced at 1 ft (0.3 m) on the top flange of the main girders supporting the deck. In addition, two C6×8.2 steel channels were placed in between the two steel girders to limit the girders' out-of-plane rotation. To simulate the restraint continuity presented in bridge decks, C-channels were placed around the outside perimeter of the experimental deck. The main deck reinforcement bars were attached manually to the surrounding C-channels to represent reinforcement continuity of an actual bridge deck. The dimensions and size of the experimental bridge deck setup were scaled to a representative size because of limited laboratory space.

Figure 1. Photo. Deck before the pour.

Figure 2. Photo. Concrete deck after the pour.

Strain Gauges and Temperature Thermocouples

The experimental bridge decks were instrumented with multiple strain gauges to measure the strain due to concrete shrinkage. Strain gauges were attached longitudinally and transversely to the main deck's reinforcing bars. Strain gauges were given a protective coating recommended by the manufacturer to protect potential damage during concrete pouring. Strain gauges were interspersed

within the center portion of the deck to collect shrinkage strains. The location of the strain gauges (foil and temperature gauges) were installed exactly at the same locations as in the previous two phases, except some extra strain gauges (marked in red) that were added to this phase. The additional foil gauges were installed to achieve a better understanding of shrinkage strain changes within the deck and to provide more information for validating the finite-element models. The intent was to instrument as much of the deck reinforcement as possible but, at the same time, not interfere with the bond between concrete and reinforcement.

In the top layer of the reinforcement mat, 20 strain gauges were attached longitudinally to reinforcing bars and 10 strain gauges were attached transversely to reinforcing bars (Figure 3). In addition, in the bottom reinforcement layer, 10 strain gauges were attached longitudinally to reinforcing bars and four strain gauges were attached transversely to reinforcing bars (Figure 4). In this experimental setup, more strain gauges were attached to the top reinforcement layer than the bottom layer. Generally, more cracks were visible on the top portion of the bridge decks because of early-age shrinkage, and those cracks mostly initiated from the top layer of reinforcement. Three strain gauges were attached to the main girder to monitor the effect of steel girders on concrete shrinkage (Figure 5). Four thermocouples were placed on the concrete deck top surface (T1), bottom surface (T2), top rebar (T3), and bottom rebar (T4) to monitor the temperature in the experimental deck immediately after concrete pouring and during concrete hardening (Figures 3 through 5).

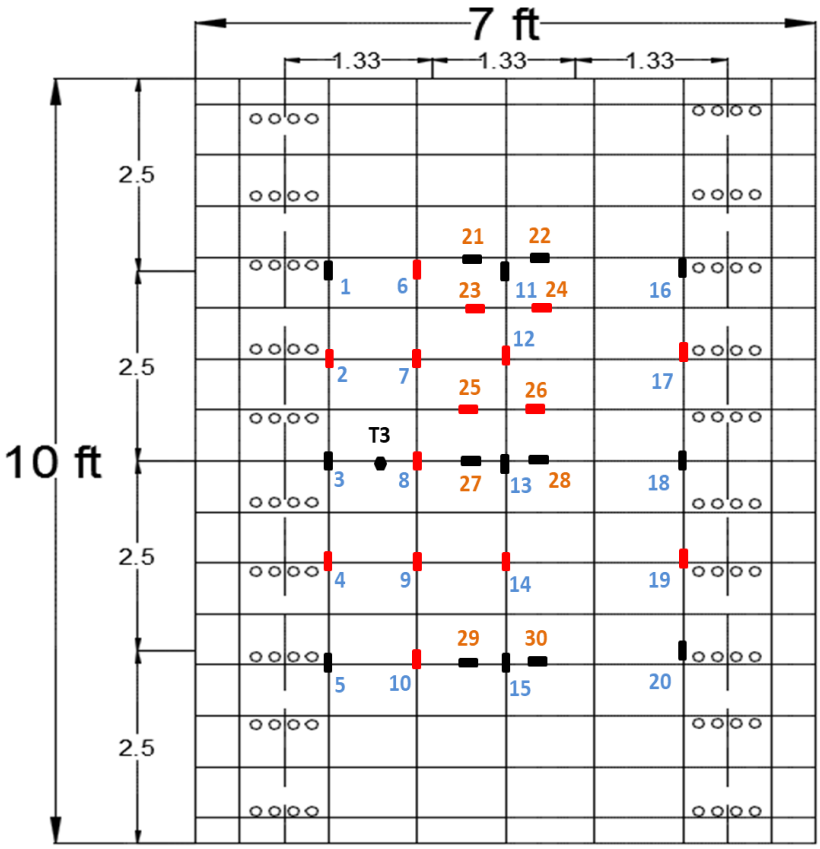

Figure 3. Illustration. Strain gauge location on top rebars.

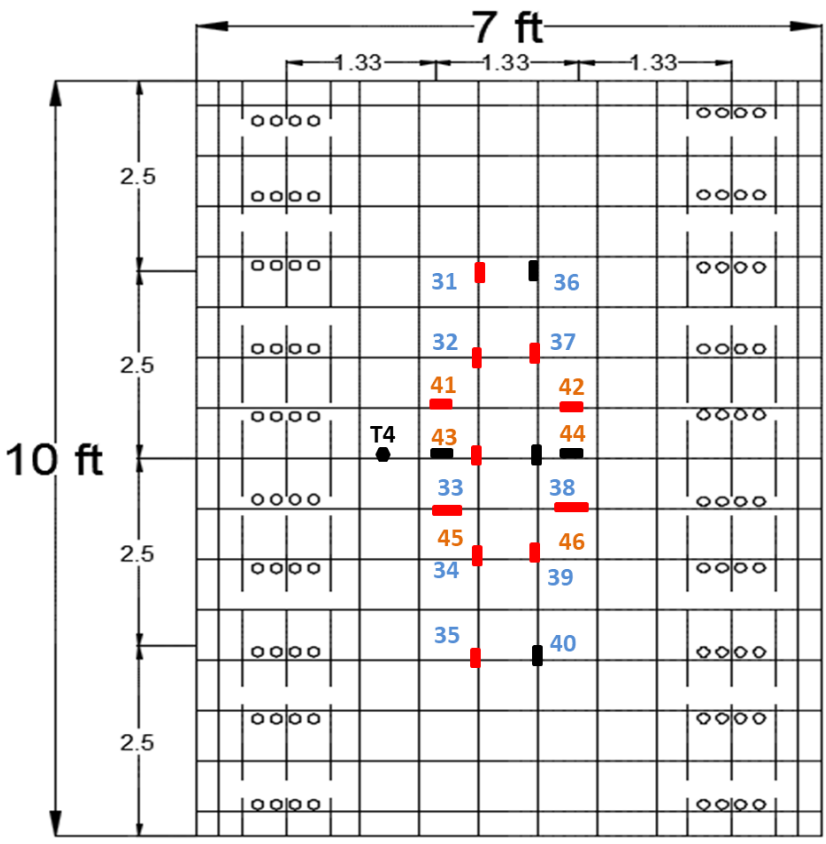

Figure 4. Illustration. Strain gauge location on bottom rebars.

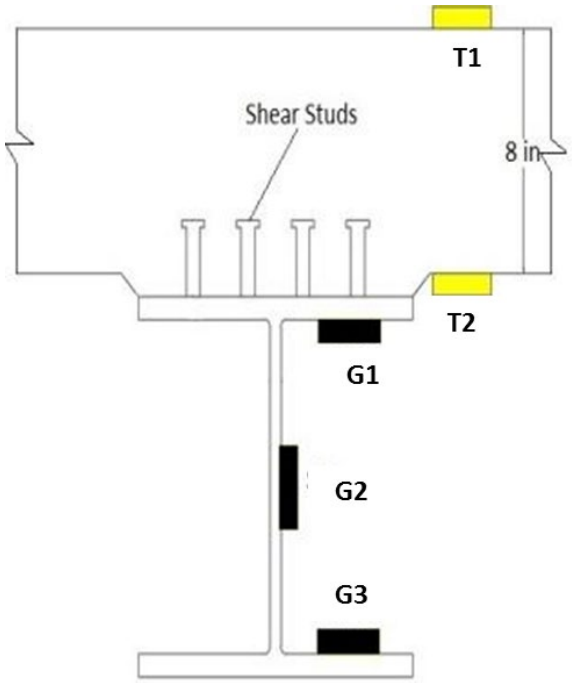

Figure 5. Illustration. Girder strain gauge (G) and thermocouple (T) layout.

Vibrating Wire Strain Gauges

In addition to the foil strain gauges, 14 vibrating wire strain gauges (VWSG) were added to measure the strain change within the concrete. VWSG (Geokon Model 4200) were placed in two different directions, as shown by the blue circle and red triangle in Figure 6. Eight VWSG were attached longitudinally to reinforcing bars and seven VWSG were attached transversely to reinforcing bars. Usually, concrete and reinforcement strain were assumed to be the same (i.e., it was assumed that concrete and reinforcement are fully bonded). Therefore, the vibrating wire strain gauges were added to allow investigation of the concrete strain and a comparison of the difference between the strain in the concrete and the reinforcement.

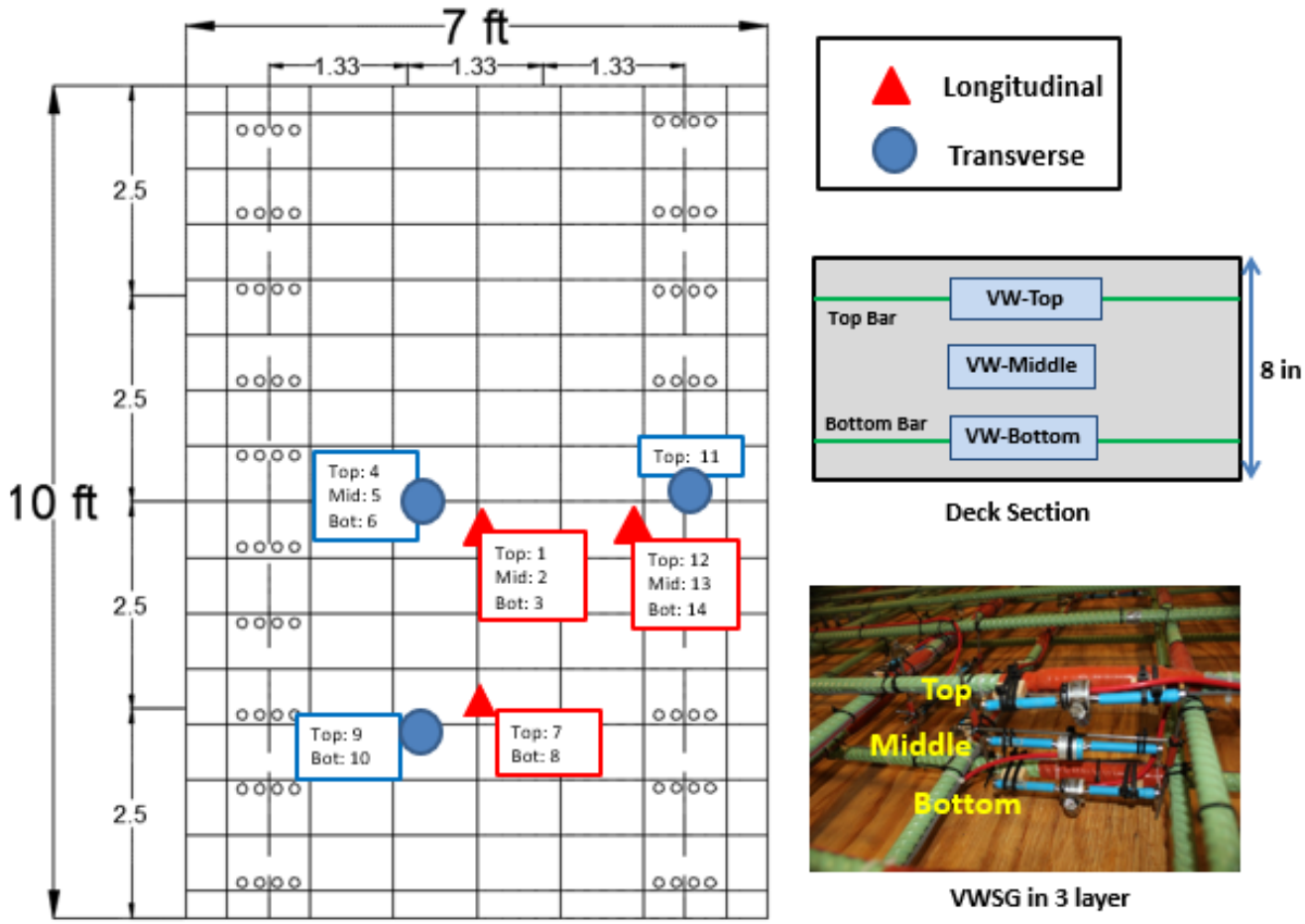

Figure 6. Illustration. Vibrating wire strain gauge location.

All VWSG as well as foil and strain gauges were connected to multiplexers (Campbell Scientific AM16/32B). The multiplexers were connected to a data-acquisition system (Campbell Scientific CR3000) to collect and monitor real-time data. The research team mimicked the experiments that were conducted in Phases I and II to have a comparable database, as seen in the "Shrinkage Strain Comparison between Mixtures" section of this report.

MIX DESIGN

Table 1 shows the proportions of all concrete mixtures included in Phases I, II, and III. In this study, three large-scale experimental decks were poured with different shrinkage-mitigating mixtures.

Two scaled bridge decks were poured with control and Type K mixtures in Phase I (Chaunsali et al., 2013). The first experimental deck was poured with 610 lb/yd^3 of Portland cement based on IDOT's standard mixture design (Rahman et al., 2018; Richardson et al., 2014). The second experimental deck was poured with partial replacement of Portland cement with expansive Type K cement. The Type K mixture was prepared by replacing a proportion of the Portland cement with Type K cement and fly ash. The Type K cement and fly ash replacement ratios were 15% and 10% (by weight), respectively.

Table 1. Mix Design, lb/yd^3

	Phase I		Phase II		Phase III		
	Control	**Type K**	**LWA**	**SRA**	**Type K + LWA (I)**	**Type K + LWA (II)**	**Type K + Gypsum**
Type I/II Cement	610	455	455	459	455	435	455
Type K Cement	-	90	-	-	90	90	90
Class C Fly Ash	-	60	155	152	60	60	60
Gypsum	-	-	-	-	-	-	6
Coarse Aggregate	1826	1829	1827	1800	1785	1823	1829
Fine Aggregate	1130	1121	712	1184	750	814	1121
SRA** (2% of cementitious material)	-	-	-	1.41	-	-	-
Water	268	272	250	251	262	240	272
Expanded Shale LWA	-	-	275.50	-	245	266	-
LWA Replacement	-	-	37%	-	33%	33%	-
Total Moisture	-	-	-	-	-	25.22%	-
Absorbed Moisture	-	-	20%	-	22%	16.88%	-
LWA Surface Moisture	-	-	9%	-	4%	9.34%	-
w/c	0.44	0.45	0.41	0.41	0.43	0.41	0.45
w/c (considering water from LWA and SRA)	-	-	0.45 (LWA)	0.44 (SRA)	0.45 (LWA)	0.45 (LWA)	-

*Units: lb/yd3 (1 lb/yd3 = 0.59 kg/m3)

**Units: gal/yd3 (1 gal/yd3 = 4.95 L/m3)

Two additional scaled bridge decks were poured in Phase II. Lightweight aggregate (LWA) and shrinkage-reducing admixture (SRA) were added to investigate their effect on overall shrinkage behavior (Ardeshirilajimi et al., 2016; Rahman et al., 2019). The lightweight fine aggregate had 20% absorption moisture and 9% surface moisture. Additional surface moisture from LWA was added to

measure an equivalent total water-to-cement (w/c) ratio of 0.45 compared to the control mixture. The second experimental deck in Phase II was poured with SRA (Ardeshirilajimi et al., 2016; Rahman et al., 2020). SRA was added as 1.41 gal/yd^3 to the concrete mixtures (2% of the cementitious material weight).

In Phase III, three different concrete mixtures were prepared with a combination of Type K cement, LWA, and gypsum mineral. Concrete mixtures were designed to accumulate the combined benefit from individual mitigating concrete from previous phases.

Three experimental decks were evaluated with the combined mixtures: Type K+LWA (I), Type K+LWA (II), and Type K+Gypsum (Table 1). Type K cement enhances early-age expansion while internally cured lightweight aggregate slowly releases the absorbed water and slows the shrinkage rate (Rahman et al., 2019). Two concrete mixtures were developed by combining expansive Type K cement and internally cured LWA: Type K+LWA (I) and Type K+LWA (II). The difference between the two mixtures was the amount of water and quality control. The Type K+LWA (II) mixture was closely observed in the ready mixture plant and the amount of extra water added in the LWA was closely measured. Quality control is important in the Type K+LWA mixture because extra water from the internally cured LWA significantly changes the early-age expansion of Type K cement. For example, LWA has various moisture contents (at the time of batching and at the time of mixing) that might affect the mixture's properties.

The Type K+LWA (I) mixture had the same total cementitious material content as the Type K mixture. The LWA replacement with fine aggregate was 33% and the adsorbed moisture content for LWA was 22%. In addition, the second Type K+LWA (II) mixture was prepared the same way as the first, except the total paste content was reduced to 26% (Type I/II cement 435 lb/yd^3). The moisture content in Type K+LWA (II) was closely and accurately measured both in the laboratory and in the ready-mixture plant before concrete pouring. The moisture content was measured following Illinois Test Procedure ICC-1. The total, absorbed, and surface moistures were 25.22%, 16.88%, and 9.34%, respectively. Figures 7 through 10 show samples collected when measuring total and absorbed moisture in the laboratory.

The third experimental deck was poured with a combination of Type K cement and gypsum mineral (Type K+Gypsum). Proper expansion is necessary at an early age for expansive cement for long-term notable reduction in concrete shrinkage. The inclusion of fly ash and expansive cement in concrete mixtures reduces early-age expansion because of the lack of adequate amount of gypsum. Gypsum is a mineral that plays an important role in controlling the rate of cement hardening. The addition of gypsum with fly ash increases the compressive strength and the durability of stabilized fly ashes. Gypsum is a hydrated calcium sulfate in a chemical form, and the addition of gypsum in the mixture significantly regulates the setting time of cement. During the cement-hydration process, gypsum quickly reacts with tricalcium aluminate (C3A), generates calcium sulfoaluminate hydrate, and constructs a protective cover on the cement particles to hinder the hydration of C3A and delay the setting time of cement. The addition of gypsum in the Type K mixture could possibly enhance early-age expansion by delaying the setting time of concrete.

Figure 7. Photo. Total moisture sample.

Figure 8. Photo. Total moisture sample in an oven.

Figure 9. Photo. Trail 1 for absorbed moisture.

Figure 10. Photo. Trail 2 for absorbed moisture.

FRESH AND HARDENED CONCRETE TEST RESULTS

The concrete's fresh properties (slump and air content) were monitored during pouring and were recorded over the one-hour pouring duration. Compressive strength tests were performed on 6 x 12 in. cylinders 7, 14, and 28 days after concrete placement in accordance with ASTM C39. The plastic properties of individual mixtures are discussed in the Phase II report (Ardeshirilajimi et al., 2016).

The Type K+LWA (I) combined mixture had an initial slump of 3.75 in. (9.52 cm) and a final slump of 5.25 in. (13.33 cm) over the one-hour pouring duration (Table 2). Two air-content tests were conducted at the beginning and end of the placement, with air contents of 4.4% and 4.5%, respectively (Table 3). The 28-day compressive strength for the Type K+LWA (I) deck was 5,557 psi (38.31 MPa) (Table 4).

These concrete tests were repeated for the deck containing the Type K+LWA (II) mixture. The initial and final slumps were 3.5 in. (8.89 cm) and 3.8 in. (9.65 cm), respectively (Table 2). Meanwhile, two air-content tests were conducted at the beginning and end of the placement, with air contents of 5.0% and 4.75%, respectively (Table 3). The 28-day compressive strength was 5,857 psi (40.38 MPa) (Table 4).

The experimental deck containing Type K+Gypsum had an initial slump of 3.25 in. (8.25 cm) and a final slump of 7.6 in (19.3 cm) at the end of pouring (Table 2). Although the slump was high at the end of the placement, it was within an acceptable range. The higher final slump could be attributed to the addition of admixture because of less workability during the pouring period. The initial and final air-content values were 5.4% and 5.5%, respectively (Table 3). The 28-day compressive strength was 4,629 psi (31.91 MPa) (Table 4).

Table 2. Slump

	Phase I		Phase II		Phase III		
	Control	Type K	LWA	SRA	Type K + LWA (I)	Type K + LWA (II)	Type K + Gypsum
Beginning of the pour	3.5	7.5	4.5	7	3.75	3.5	3.25
End of pour	2.5	7.5	7	6.5	5.25	3.8	7.6

*Units: in. (1 in. = 2.54 cm)

Table 3. Air Content

	Phase I		Phase II		Phase III		
	Control	Type K	LWA	SRA	Type K + LWA (I)	Type K + LWA (II)	Type K + Gypsum
Beginning of the pour	5.8	5.9	9.3	2.0	4.4	5.0	5.4
End of pour	6.0	5.7	7.5	2.0	4.5	4.75	5.5

*Units: % (percentage)

Table 4. Concrete Compressive Strength

	Phase I		Phase II		Phase III		
	Control	Type K	LWA	SRA	Type K + LWA (I)	Type K + LWA (II)	Type K + Gypsum
7 days	-	3030	5520	4610	4257	4259	3660
14 days	-	3690	6100	5460	4620	5205	4188
28 days	4560	4340	6990	6220	5557	5857	4629

*Units: psi (1 psi = 6,894 Pa)

STRAIN AND TEMPERATURE VARIATION IN BRIDGE DECKS

In Phases I and II, the research team investigated the implementation of Type K cement, LWA, and SRA in IDOT concrete mixtures as an effort to reduce concrete shrinkage. In the present phase of the research project, experimental work was conducted by pouring scaled reinforced concrete decks using binary mixtures of Type K cement, LWA, and gypsum. Three experimental decks were built in this phase with a combination of Type K cement, LWA, and gypsum. One of the experimental decks, Type K+LWA (I), was poured in March 2018, while another companion deck, Type K+LWA (II), was poured in November 2019. A third experimental deck, Type K+Gypsum, was poured in December 2018. All experimental decks were placed inside the laboratory to avoid environmental effects due to different casting periods and to ensure all poured desks have the same surrounding environmental conditions. All scaled decks were continuously monitored for six months.

Type K+LWA (I) Concrete Deck

The strain gauge and thermocouple setup were similar to that in Phases I and II. Similar types of strain gauges and thermocouples were used to monitor the shrinkage internal strain and temperature of the concrete deck. To eliminate initial strain due to vibration and installation, strain gauges were zeroed at 1.5 hours after concrete placement. The recorded strain from the experimental deck showed a similar trend as was reported in the previous phases of the research project. In the early age of the curing period, the strain went upward because of expansive cement hydration. After a seven-day curing period, the concrete started the drying phase, and the strain moved downward because of the onset of shrinkage. Some results collected from strain gauges deviated from this general trend because of the slippage between rebar and the surrounding concrete. In this study, those deviated strains were ignored while plotting the average strain graphs.

Strain Gauge Results

The strain gauge results of the Type K+LWA (I) concrete deck are shown in Figures 11 through 14. The individual strain in the top reinforcing bars for the longitudinal and transverse directions is shown in Figures 11 and 12, respectively. Figure 11 shows the top longitudinal strain with a peak between 150 με to 205 με at seven days. At the end of the drying period, shrinkage strain was between −50 με to −230 με at 182 days. Figure 12 shows the transverse strain in the top bars, where the peak strain was around 280 με at seven days and between −190 με to −210 με at the end of the drying period. The bottom longitudinal reinforcement peak strain was around 190 με at seven days, and the strain at the end of six months was between −50 to −120 με (Figure 13). During the concrete placement, all gauges that were attached to the bottom transverse reinforcement were lost.

The strain reading on the top flange of the steel girder (gauge location as shown in Figure 5) showed the same trend as for concrete (Figure 14). The strain reading showed expansion during the hydration period followed by shrinkage during the drying period. The strain at the middle of the beam web followed a similar trend as the top flange with a lower rate. The strain reading on the bottom flange showed the opposite sign compared to the top flange strain due to bending induced from concrete shrinkage (Figure 14).

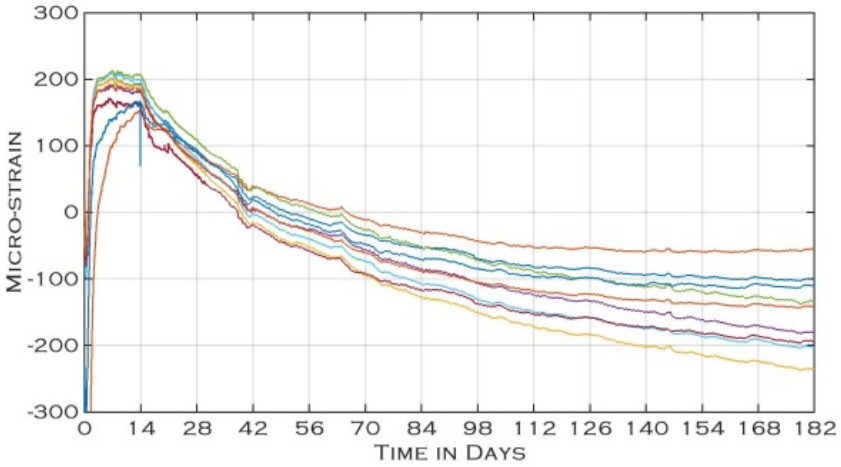

Figure 11. Graph. Top longitudinal strain.

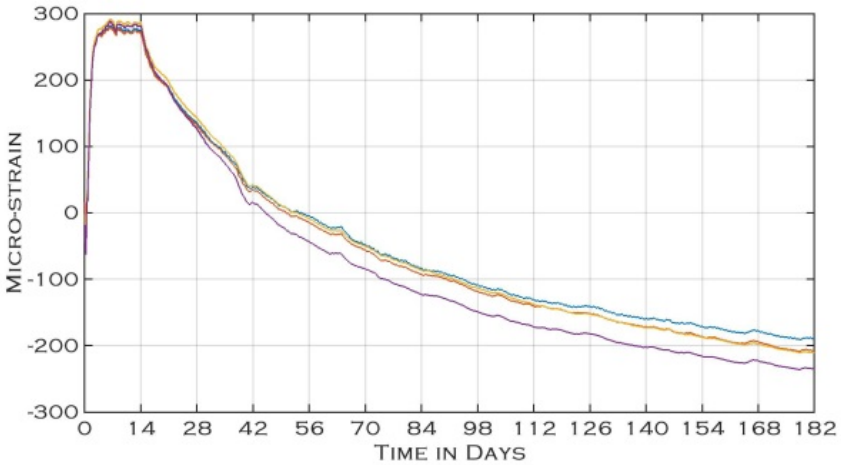

Figure 12. Graph. Top transverse strain.

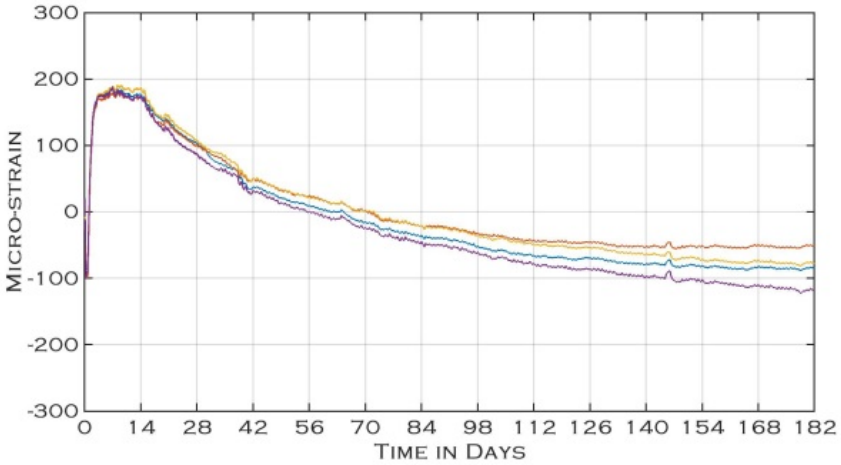

Figure 13. Graph. Bottom longitudinal strain.

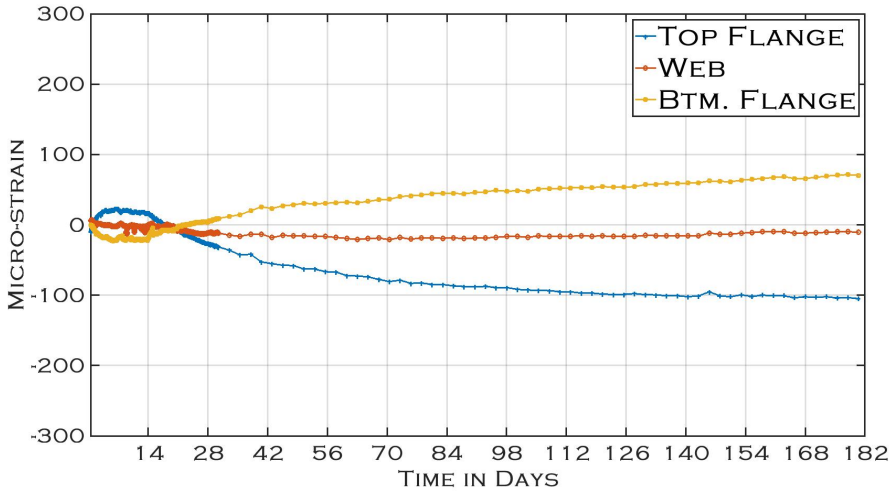

Figure 14. Graph. Girder strain.

Thermocouple Results

Figure 15 shows the thermocouple reading for the Type K+LWA (I) deck. Four thermocouples were placed through the deck thickness (locations as shown in Figures 3 through 5) to track the temperature changes along the deck depth, and temperature did not need to be zeroed like the strain gauge reading.

The temperature within the Type K+LWA (I) concrete mixture reached 100°F (37.7°C) approximately 24 hours after concrete placement. After 14 days, the temperature of the top and bottom surfaces of the deck showed similar readings (with no significant differences) compared to the top and bottom reinforcement bar locations. The temperature reading was consistent through the deck thickness because the deck was placed in a well-confined environment.

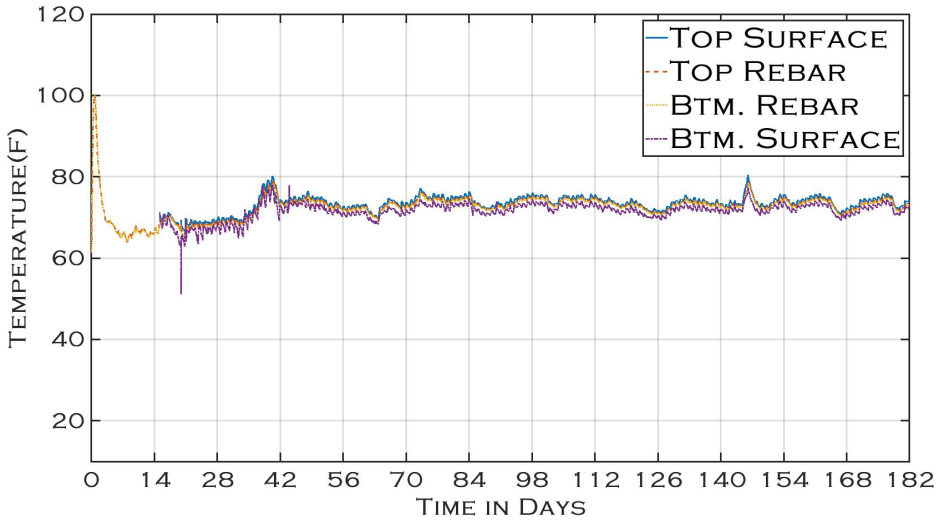

Figure 15. Graph. Temperature-time history.

Vibrating Wire Strain Gauge Readings

The strain measurement collected from the vibrating wire strain gauges (concrete gauges) for the Type K+LWA (I) deck are shown in Figures 16 through 19. The VWSG strain in the longitudinal and transverse directions is shown in Figures 16 and 17, respectively. The peak concrete strain was similar compared to the strain collected from foil strain gauges. Figure 18 shows the VWSG #1 strain compared with the foil strain gauge reading from the same reinforcement location. The measured strain showed almost identical values from this location for both the VWSG and foil gauges. This comparison shows a similar trend of strain values between reinforcement and concrete at that location. Figure 19 shows a similar trend for the foil and VWSG strain comparison.

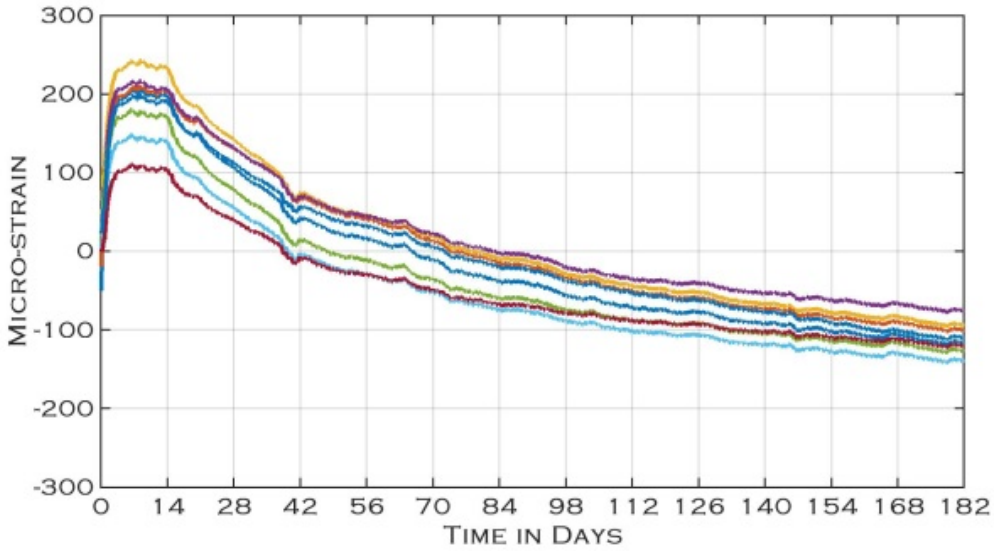

Figure 16. Graph. All longitudinal VWSG strain.

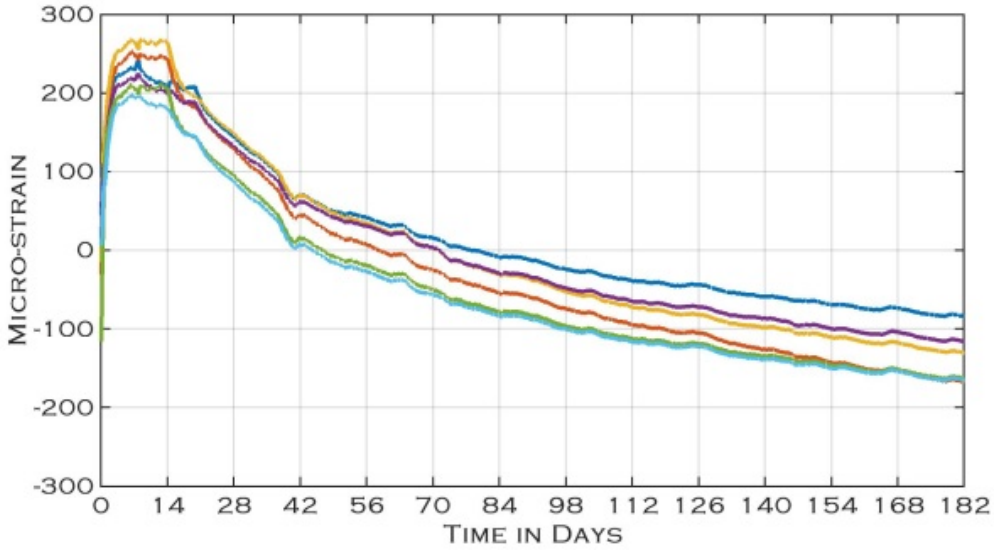

Figure 17. Graph. All transverse VWSG strain.

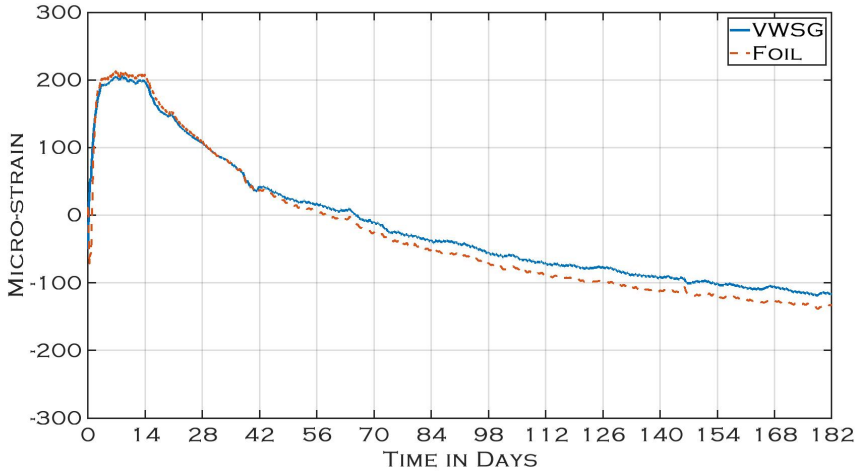

Figure 18. Graph. VWSG (#1) and foil gauge (#13) strain comparison from the same location.

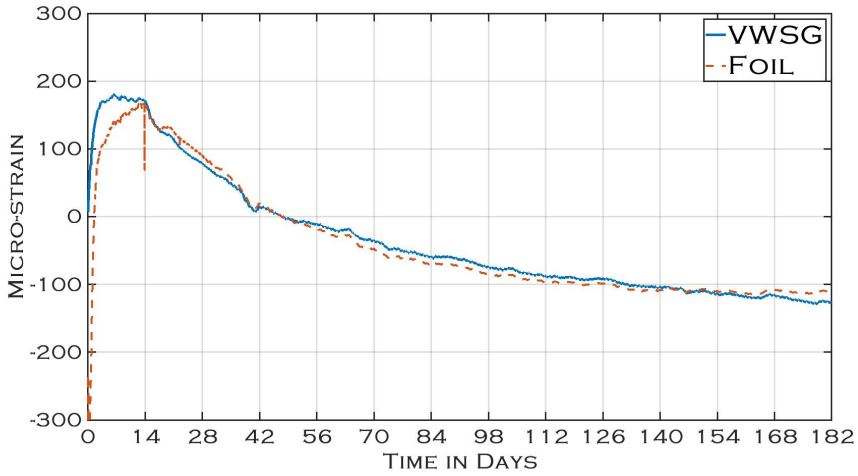

Figure 19. Graph. VWSG (#12) and foil gauge (#18) strain comparison from the same location.

Type K+LWA (II) Concrete Deck

The second combined mixture of Type K cement and lightweight aggregate (LWA) was investigated with a different water-to-cement (w/c) ratio, as explained in the "Mixture Design" section (Table 1). The amount of water from LWA was closely and accurately measured to understand the effect of the additional water provided by the prewetted LWA on early-age expansion.

Strain Gauge Results

The strain results of the experimental deck poured with the Type K+LWA (II) concrete mixture are shown in Figures 20 through 23. The monitored strain from this experimental deck showed the same trend as the Type K+LWA(I) mixture. At an early age, the strain increased due to cement hydration followed by drying shrinkage, while the strain started to decrease around seven days. Strain in the top reinforcement layer for longitudinal and transverse directions is shown in Figures 20 and 21,

respectively. The peak strain was between 110 to 205 με in the top longitudinal direction at seven days and was between −95 to −200 με at the end of six months (Figure 20). One longitudinal foil gauge showed a different strain trend compared to other gauges. Initially, the measured strain from that gauge followed a similar expansion and then by drying until 42 days. After 42 days, that gauge showed an upward trend with an increase in the strain value. This could be due to an internal crack at that location. The transverse strain on top reinforcement had a peak strain between 200 to 250 με, and the strain at the end of six months was between −100 to −195 με (Figure 21). In the top transverse direction, two of the strain gauges also showed different trends compared to other strain values, which could possibly indicate cracks at those locations. However, there were no cracks found on the top surface of the experimental deck poured with the Type K+LWA (II) mixture.

The strain in the bottom longitudinal reinforcement had a peak between 110 to 150 με, and the shrinkage strain was between −60 to −120 με at the end of six months (Figure 22). The bottom transverse layer had a peak strain around 150 με, and the strain at the end of six months was between −95 to −195 με (Figure 23).

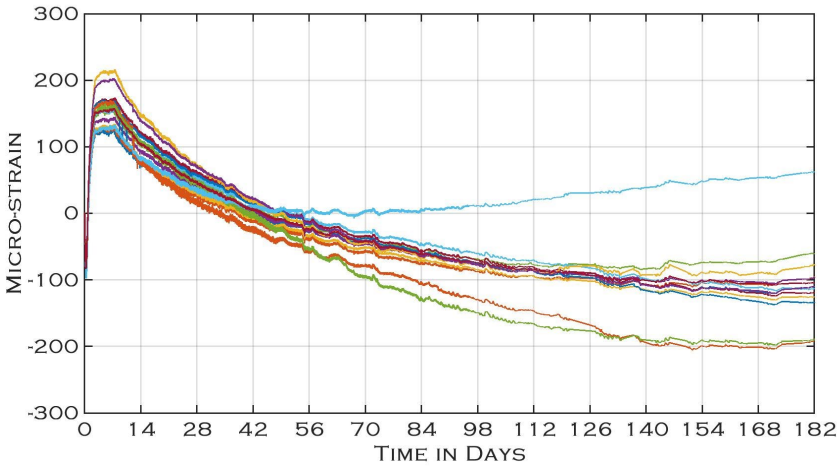

Figure 20. Graph. Top longitudinal strain.

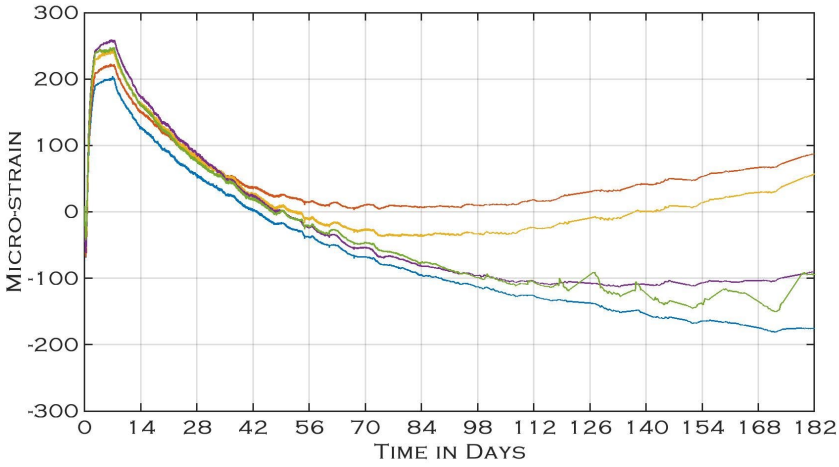

Figure 21. Graph. Top transverse strain.

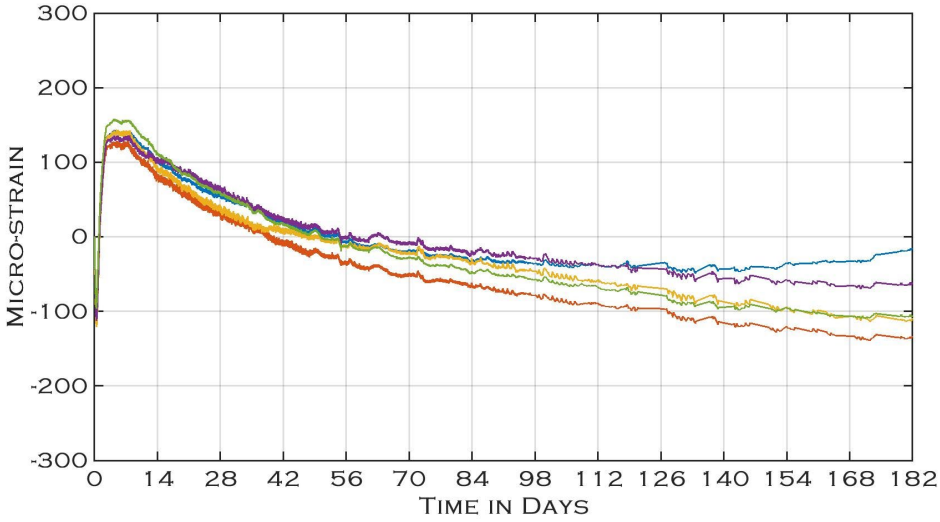

Figure 22. Graph. Bottom longitudinal strain.

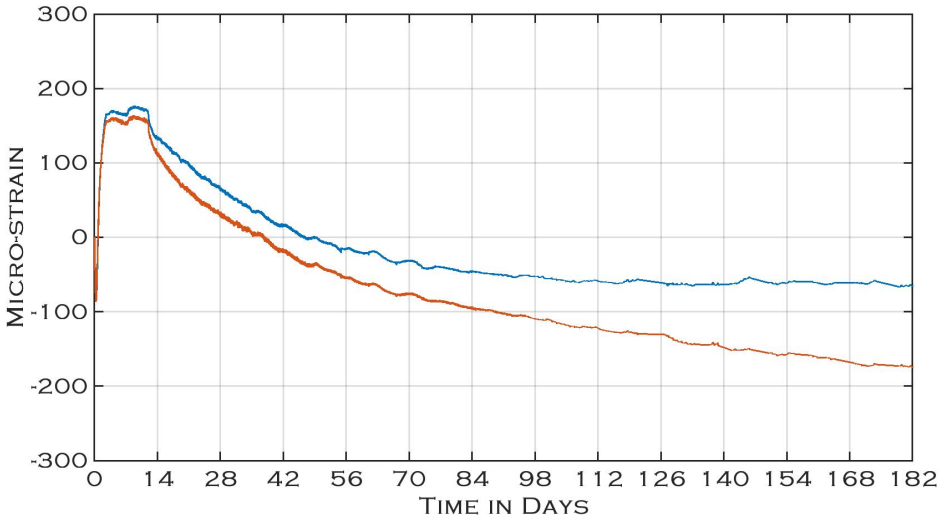

Figure 23. Graph. Bottom transverse strain.

Thermocouple Results

Similarly, as in Phases I and II, four thermocouples were placed inside the Type K+LWA (II) experimental deck as well. Figure 24 shows the thermocouple reading for the Type K+LWA (II) deck. The internal temperature reached 90°F (32.2°C) approximately 24 hours after concrete placement. Figure 24 shows a consistent temperature difference between the top and bottom deck surfaces and rebar.

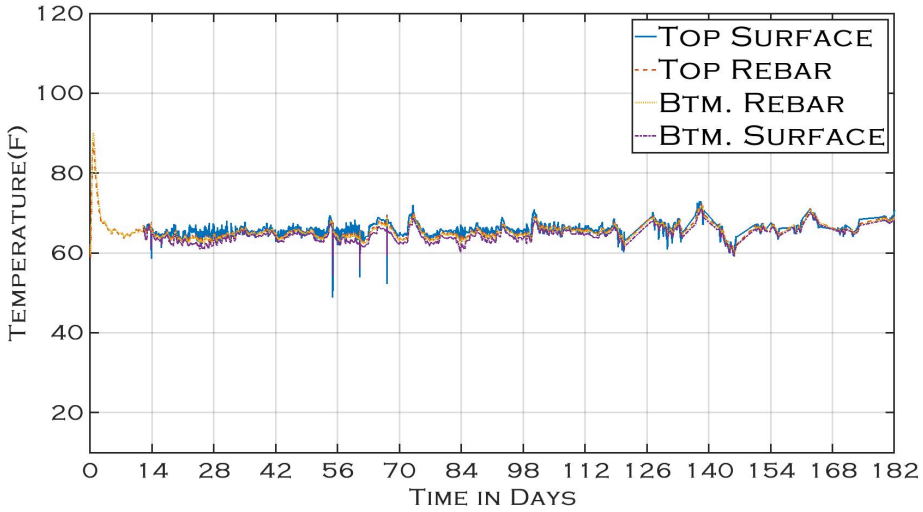

Figure 24. Graph. Temperature-time history.

Vibrating Wire Strain Gauge Readings

The strain collected from the vibrating wire strain gauges (concrete gauges) for the Type K+LWA (II) deck are shown in Figures 25 through 28. The VWSG strains in the longitudinal and transverse directions are shown in Figures 25 and 26, respectively. The peak concrete strain in the longitudinal and transverse directions shows a similar value compared with the foil gauge strain at seven days. At the end of the drying period, the average VWSG strain also has a similar value compared with the foil gauges. Figures 27 and 28 show the comparison between foil and VWSG strain at the same reinforcement locations. In both graphs, VWSG and foil gauges have a similar strain value over the drying period.

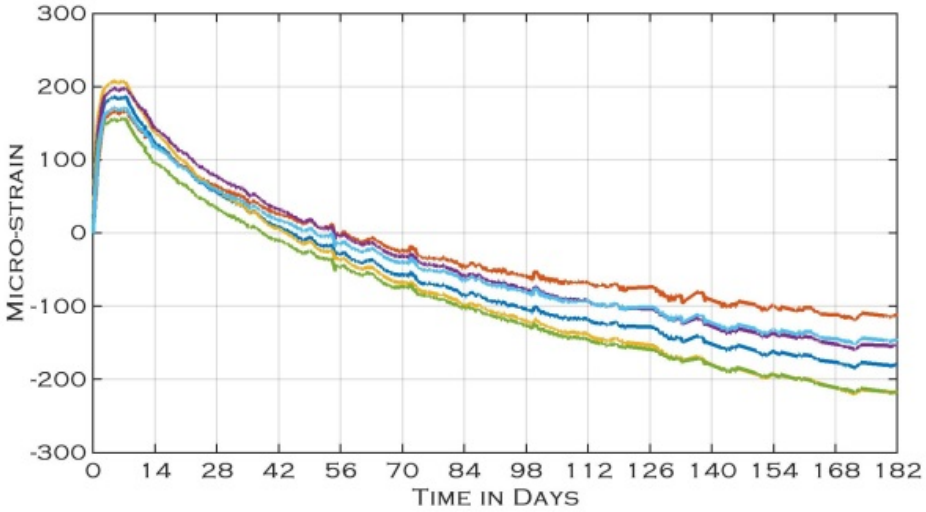

Figure 25. Graph. All longitudinal VWSG strain.

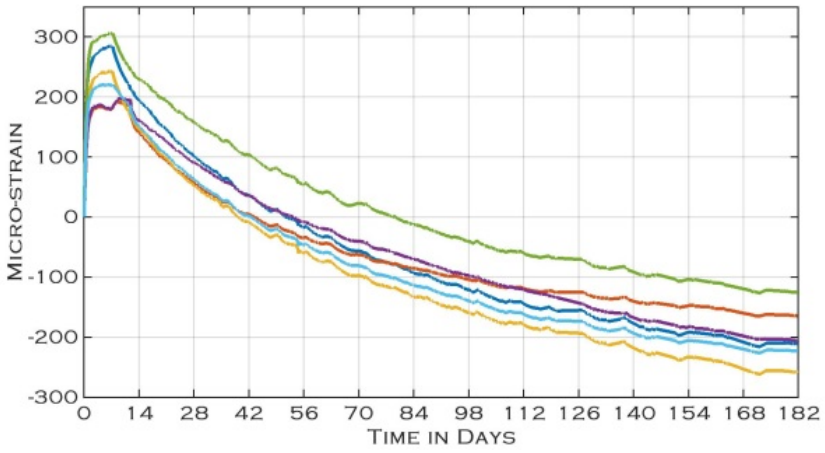

Figure 26. Graph. All transverse VWSG strain.

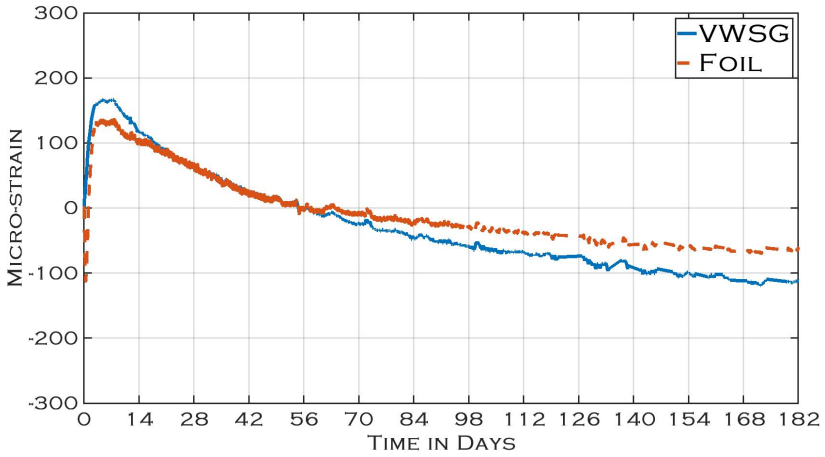

Figure 27. Graph. VWSG (#3) and foil gauge (#38) strain comparison from the same location.

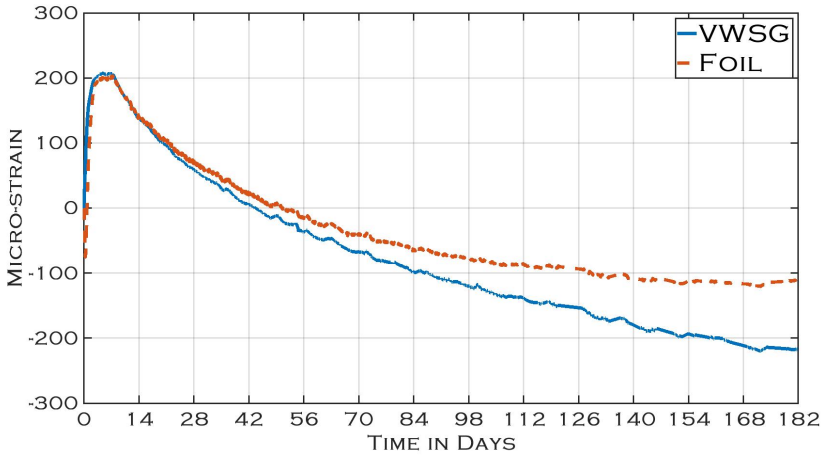

Figure 28. Graph. VWSG (#7) and foil gauge (#15) strain comparison from the same location.

Type K+Gypsum Concrete Deck

The third experimental deck in this phase was investigated with the combined Type K and gypsum mineral (Type K+Gypsum). Numerous efforts have focused on reducing concrete early-age cracking by improving various shrinkage-mitigating concrete mixtures (Arezoumandi, 2015; Hadidi & Saadeghvaziri, 2005). The use of expansive cement in concrete decks reduces cracking by early-age expansion. Gypsum was added with the Type K cement to investigate the effect of such binary mixture combination in reducing shrinkage of concrete in bridge decks. Enhancing early-age expansion of Type K cement with the addition of gypsum plays a significant role in creating an initial compressive stress inside the concrete that could reduce cracking possibility in bridge decks. The use of gypsum with Type K cement and in the existence of class C fly ash has reduced early cracking to concrete mixtures compared to other SCMs. Gypsum inhibits class C fly ash to consume ye'elimite (hydration product of Type K). The scaled deck was made to investigate the behavior of Type K+Gypsum concrete mixtures in a closer scale to reality.

Strain Gauge Results

The recorded strain for the Type K+Gypsum experimental deck follows a similar trend as the results of the previous deck. Figures 29 through 32 show the strain inside the Type K+Gypsum experimental deck.

The peak strain in the top longitudinal direction was between 95 to 140 με at seven days and was between −190 to −280 με at the end of six months (Figure 29). One of the longitudinal foil gauges (shown in red in Figure 29) showed an upward strain after 28 days compared to other strain gauges. During the hydration period, that gauge showed an expansion similar to other gauges, and after 28 days, the upward strain indicated a possible crack at the strain gauge location. Similarly, another strain gauge showed an upward trend (shown in green in Figure 29) after 100 days, which also indicates a possible internal crack on that specific strain gauge location. The transverse strain on the top reinforcement has a peak strain between 130 to 180 με at seven days, and the strain at the end of six months was between −230 to −280 με (Figure 30).

The strain in the bottom longitudinal reinforcement had a peak between 85 to 105 με, and the shrinkage strain was between −100 to −205 με at the end of six months (Figure 31). The bottom transverse layer has a peak strain around 100 με at seven days, and the strain at the end of six months was between −180 to −205 με (Figure 32).

All gauges installed on the girder were lost for this experimental deck because of either a water leakage inside the strain gauges or a malfunctioning connection between the multiplexer and datalogger.

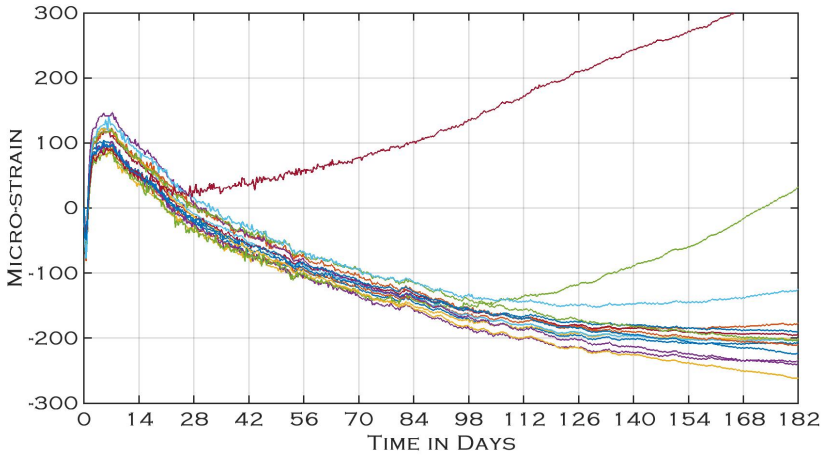

Figure 29. Graph. Top longitudinal strain.

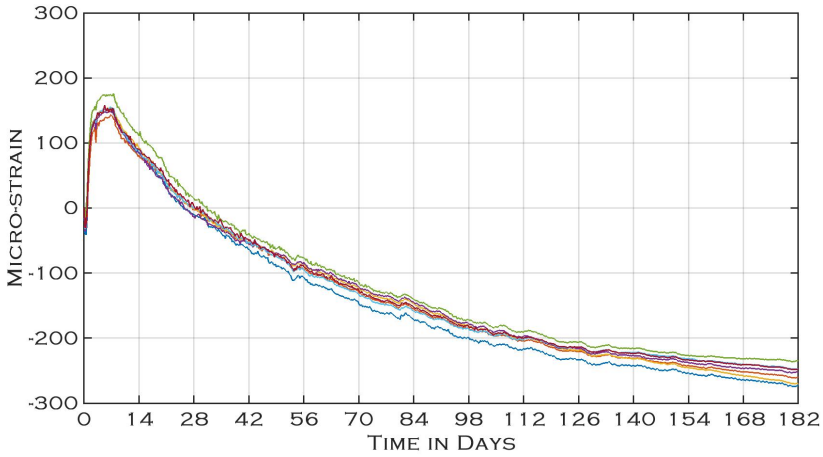

Figure 30. Graph. Top transverse strain.

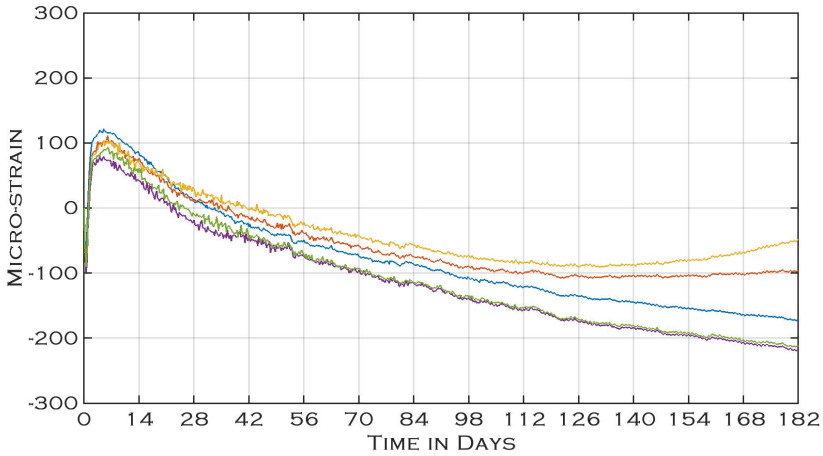

Figure 31. Graph. Bottom longitudinal strain.

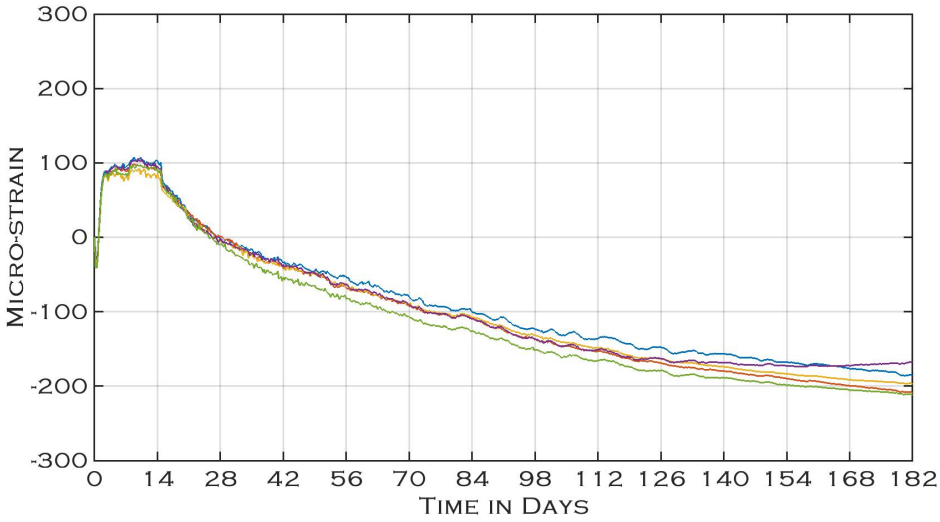

Figure 32. Graph. Bottom transverse strain.

Thermocouple Results

Figure 33 shows the thermocouple results for the Type K+Gypsum experimental deck. Four thermocouples were installed inside the concrete deck with the same location as previous decks. Thermocouple measurements inside the Type K+Gypsum deck showed a peak temperature of around 102°F (38.8°C) at 24 hours after placement. The deck was built inside a laboratory with a controlled environment and followed similar steps as previous decks. As shown in Figure 33, thermal variation is insignificant between the surfaces and reinforcement layers.

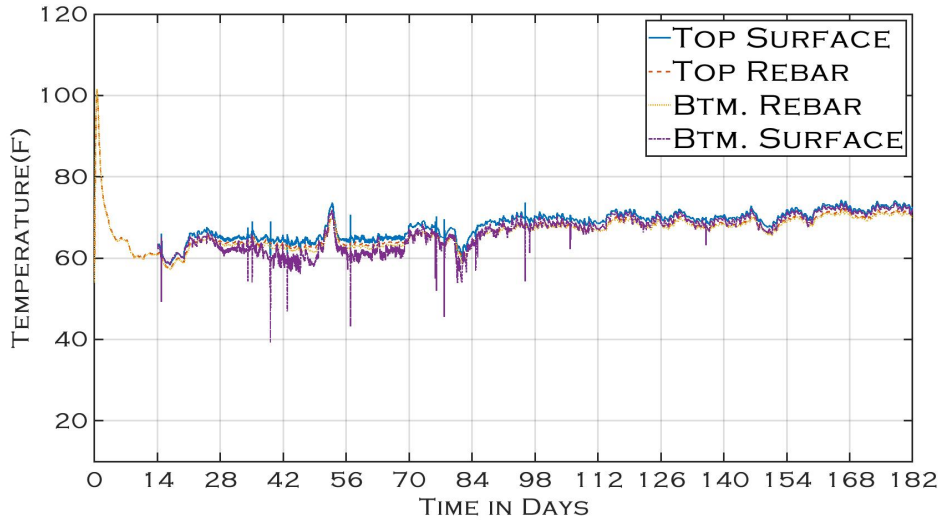

Figure 33. Graph. Temperature-time history.

Vibrating Wire Strain Gauge Readings

The strain measurement collected from the vibrating wire strain gauges (concrete gauges) for the Type K+Gypsum deck are shown in Figures 34 through 37. The VWSG strains in the longitudinal and transverse directions are shown in Figures 34 and 35, respectively. The peak concrete strain is similar to the strain collected from foil strain gauges. At the end of the drying period, the average VWSG strain also has a similar value compared to foil gauges. Figure 36 shows the VWSG #1 strain compared with the foil strain gauge reading from the same reinforcement location. Figure 37 shows the strain comparison between a concrete gauge (VWSG#7) and foil gauges from the same reinforcement location. Figure 37 shows a strain difference between foil and concrete gauges. Meanwhile, a corresponding concrete gauge (VWSG#7) near the foil gauge shows a general concrete shrinkage trend. This could be due to a possible crack formation at the exact location of the foil gauge.

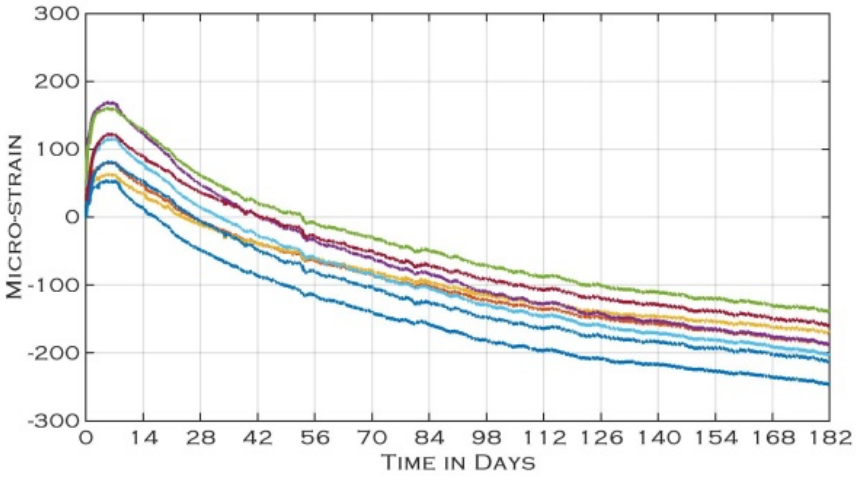

Figure 34. Graph. All longitudinal VWSG strain.

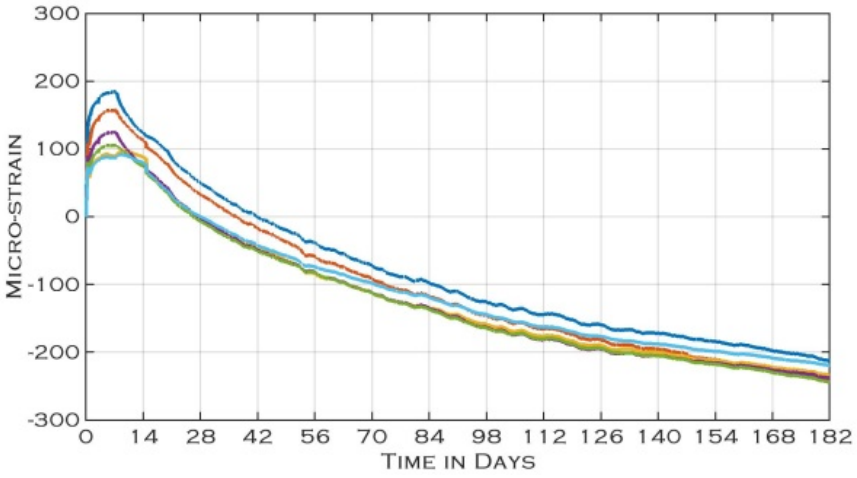

Figure 35. Graph. All transverse VWSG strain.

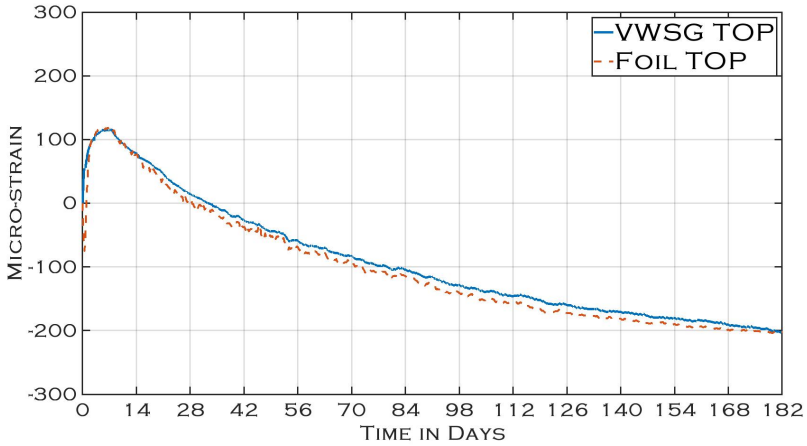

Figure 36. Graph. VWSG (#1) and foil gauge (#13) strain comparison from the same location.

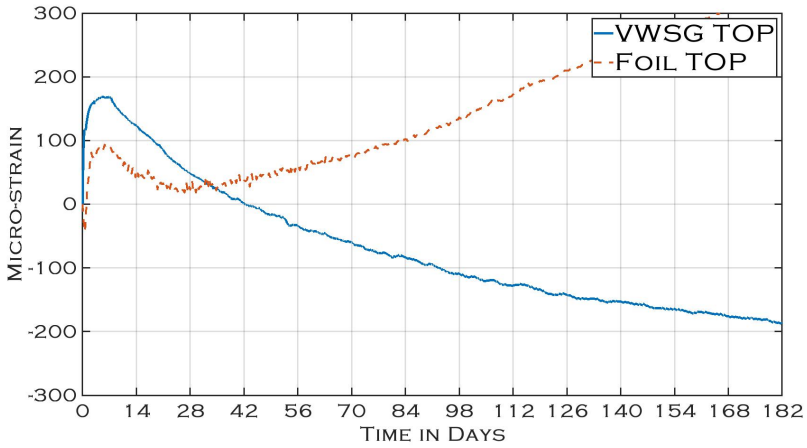

Figure 37. Graph. VWSG (#7) and foil gauge (#15) strain comparison from the same location.

SHRINKAGE STRAIN COMPARISON BETWEEN MIXTURES

Strains measured in the longitudinal reinforcement are the primary focus for this research because they represent the mechanism by which transverse cracking is initiated in the field. Shrinkage strains from all experiment decks were plotted together to understand the restrained drying shrinkage behavior of different concrete mixtures (Figures 38 through 41). Some strains appeared to deviate from this general trend due to slippage between the reinforcement and concrete or due to small initial cracks developed at that location. Those off-trend strain readings were ignored while plotting the average strain time history.

The average strain measured longitudinally for the top and bottom reinforcing mats is shown in Figures 38 and 39, respectively. The average peak strain in the top longitudinal direction for the control mixture was around 45 με at seven days and −195 με at the end of the drying period. The deck containing Type K cement has a higher peak than the control mixture. The average top longitudinal peak strain for the Type K mixture was around 90 με at seven days and −200 με at 182

days. The seven-day peak strain for the LWA concrete slab is 50% lower than for the control concrete. The LWA concrete specimen exhibited a slower shrinkage rate compared to the control deck. The average peak strain in the top longitudinal direction for the SRA mixture was 50 με at seven days and −50 με at the end of the drying period. The SRA concrete specimen exhibited a slower shrinkage rate compared to other mixtures. The experimental deck containing Type K+LWA (I) showed a peak value around 200 με, which is the highest peak compared to all mixtures. The average top longitudinal peak for the Type K+LWA (II) mixture is 175 με at seven days and −120 με at 182 days. The average top longitudinal peak for the Type K+Gypsum mixture is 105 με at seven days and −210 με at 182 days.

Figure 39 shows the average strain from the bottom mat in the longitudinal direction. The trend observed in the bottom mat was similar to that measured in the top mat, with a few notable differences. The total expansion was similar for each deck; however, peak values at the bottom mat occurred a few days later compared to the top reinforcement mat, as the bottom formwork was not removed for an additional seven days. This effectively increases the curing period and results in a reduction in shrinkage of anywhere from 20 to 50 με compared to the top mat.

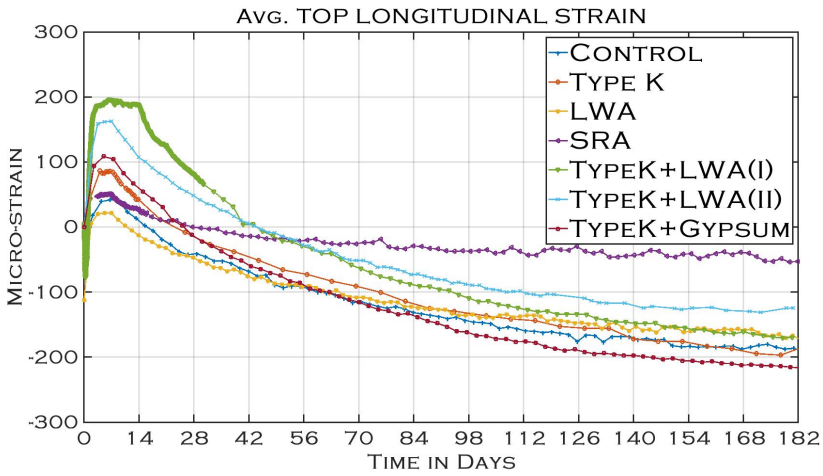

Figure 38. Graph. Average top longitudinal strain.

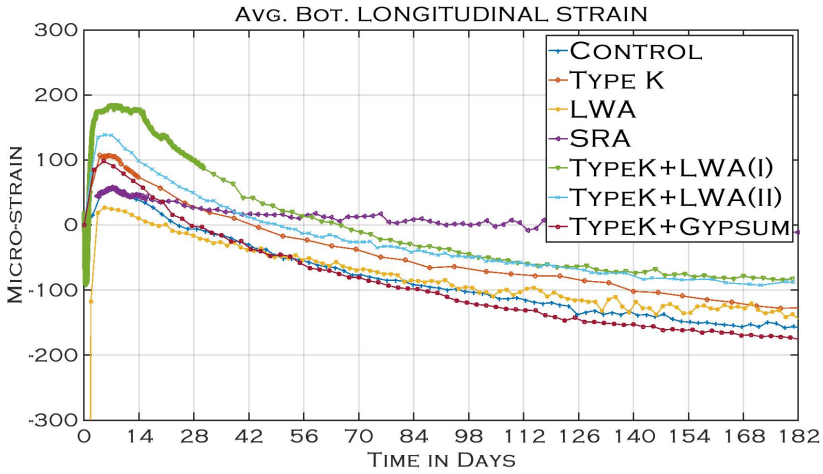

Figure 39. Graph. Average bottom longitudinal strain.

Figure 40 presents the average of all strains gauges in the longitudinal direction for different concrete mixtures and exhibits a similar trend as Figures 38 and 39. The combined mixtures of expansive cement and internally cured lightweight aggregate known as Type K+LWA (I) and Type K+LWA (II) exhibited a higher peak compared to other mixtures. The proper expansion of Type K cement was important at early days. During the hydration period, additional water from the internally cured LWA enhanced early-age expansion of Type K cement. The Type K+LWA (I) mixture had approximately 325% higher expansion at seven days and 32% less shrinkage at the end of the drying period compared to the control mixture. Similarly, a deck containing the Type K+LWA (II) mixture had approximately 238% higher expansion at seven days compared to the control mixture. The Type K+LWA (II) mixture shows less expansion compared to the Type K+LWA (I) mixture because of initial available water amount (w/c 0.41) and reduced paste content (26%). However, the Type K+LWA (II) mixture showed significantly less shrinkage (43% less) compared to the control deck at the end of the drying period. A combination of Type K and gypsum mineral (Type K+Gypsum) showed insignificantly higher expansion compared with the individual Type K mixture. The rate of shrinkage between the combined Type K+Gypsum and individual Type K mixture showed an almost similar rate. The Type K+Gypsum mixture showed slightly increased shrinkage (6%) at the end of the drying period compared to the control deck.

The mixture containing Type K cement showed 109% higher expansion compared to the control mixture during the hydration period. Although Type K has a higher expansion, it showed a similar shrinkage rate compared to the control mixture. At the end of the drying period, the Type K mixture showed a 15% reduction in shrinkage compared to the control mixture. Compared with the control mixture, LWA presents approximately 50% less expansion at seven days but also exhibits a 10% less shrinkage value at 182 days. The initial expansion for the SRA mixture showed a similar peak strain compared to the control mixture, but over time the SRA deck exhibited a slower shrinkage rate at the end of the drying period.

Figure 41 illustrates the total shrinkage for various concrete mixtures, including experimental decks from previous phases. Type K and the control mixture had a difference of 40 με at the end of the six-month monitoring period. After the hydration period, LWA slowly released absorbed water, which resulted in a slower shrinkage rate compared to the control mixture. The Type K+Gypsum mixture had a similar peak strain compared to the individual Type K mixture but had a higher shrinkage rate during the drying period. The combined Type K+LWA (I) mixture had the highest total shrinkage compared to other mixtures. This could be due to the available extra water in the mixture from internally cured LWA. Available extra water in the mixture significantly enhanced the performance of Type K cement's initial expansion; however, the available extra water in the concrete mixture possibly dried out over the drying period and caused larger total shrinkage. The deck containing SRA had the lowest total shrinkage compared to other mixtures. At the end of the six-month drying period, SRA showed 73% less shrinkage strain than the control mixture.

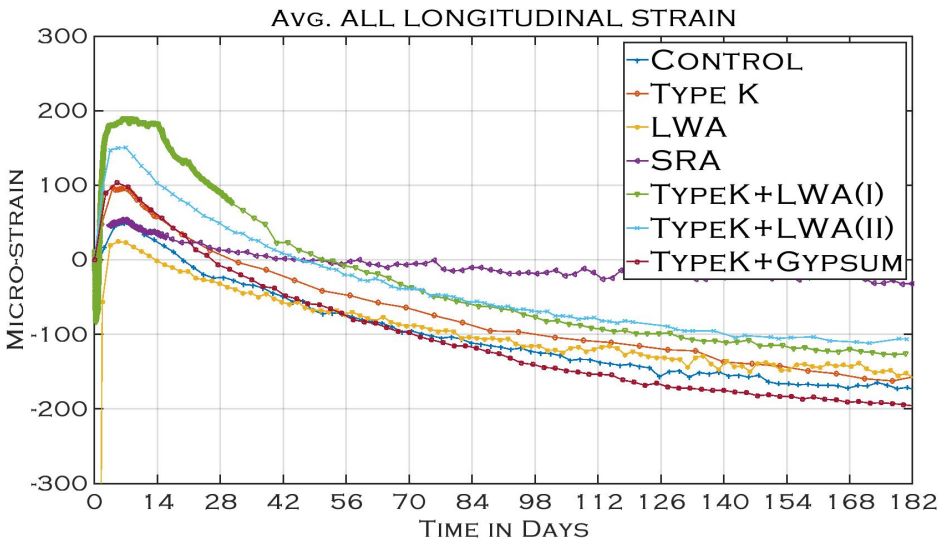

Figure 40. Graph. Average all longitudinal strain.

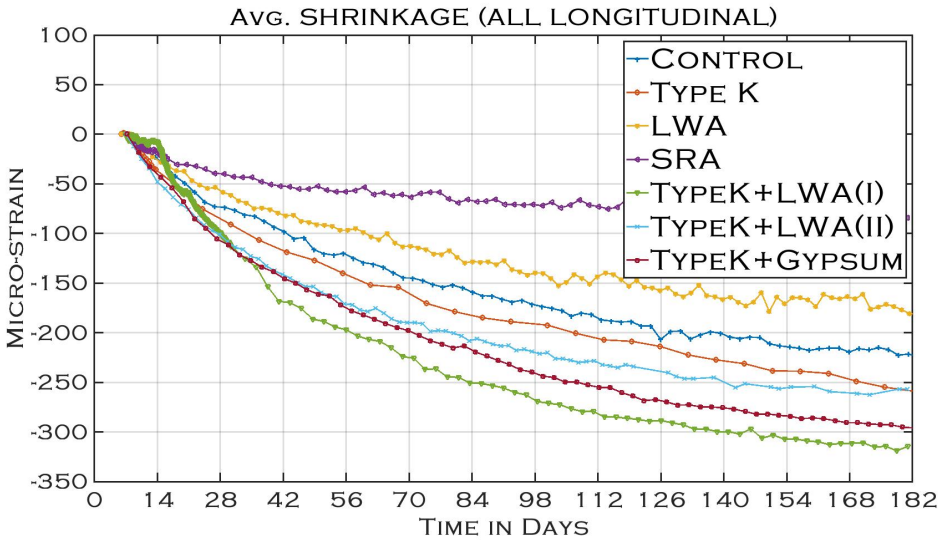

Figure 41. Graph. Average total shrinkage.

ECONOMIC ANALYSIS

This section presents the economic analysis of shrinkage-mitigating materials used to pour various experimental scaled concrete decks for all phases of this project. The average concrete cost per cubic yard for concrete including Type I/II cement (Portland) is around $90 to $100. Figure 42 shows the additional cost added by different mitigating materials on pouring concrete per cubic yard.

In this study, 90 lb of Type K expansive cement was used per cubic yard of concrete. Manufactured by CTS Komponent, one sack of expansive cement contains 90 lb of Type K cement, which adds $34 per cubic yard of concrete on top of the average concrete cost. Lightweight aggregate used for this study was manufactured from the ARCOSA Lightweight (formerly Trinity Lightweight) and added additional

$10 per cubic yard of concrete. A shrinkage-reducing admixture added $55 per cubic yard of concrete and was manufactured by GCP Applied Technology. One gallon of SRA admixture supplied from GCP Applied Technology cost $38.61 per gallon (when delivered in bulk of 500 gallons or more). In this study, additional gypsum was used with Type K cement for additional expansion. For research purposes, pure gypsum was collected from Fisher Scientific to avoid impurities. Adding gypsum results in an extra cost around $110 per cubic yard of concrete on top of costs from Type I/II and Type K cement. The price of 5.5 lb (2.5 kg) of gypsum was around $97.55, manufactured by Fisher Scientific. The cost for pure gypsum is higher than the traditional gypsum available in the market.

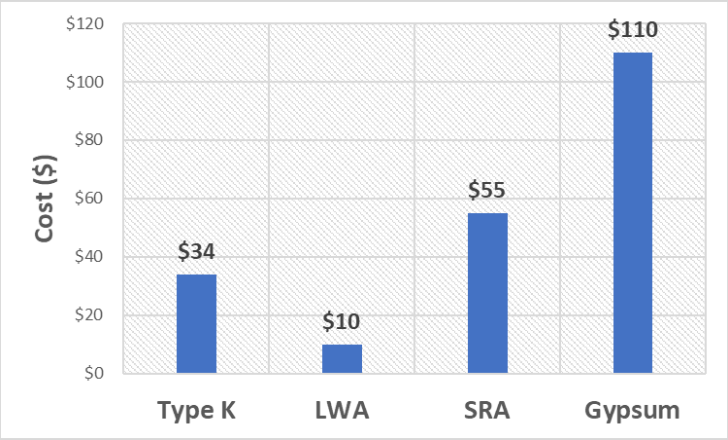

Figure 42. Chart. Added cost per yd^3 of concrete.

SUMMARY

Type K cement provided a higher expansion during early-age concrete curing. Lightweight aggregate showed a slower rate of shrinkage by releasing absorbed water. The combined mixture Type K+LWA (I) had the highest total shrinkage compared to other mixtures. Available extra water in the mixture significantly enhanced the performance of Type K cement's initial expansion; however, the available extra water in the concrete mixture possibly dried out over the drying period and caused larger total shrinkage. Overall, the SRA mixture showed a slower rate of shrinkage and ended with the least shrinkage strain at the end of the drying period compared to other mitigating mixtures.

CHAPTER 3: FINITE-ELEMENT ANALYSIS

This chapter presents shrinkage cracking through a combination of laboratory experimentation and finite-element (FE) modeling. A specific objective of this chapter is the development of a FE model that could correctly evaluate and predict the shrinkage-induced stress-strain behavior within a bridge deck. Three-dimensional FE models using Abaqus were developed to determine the overall structural response due to shrinkage.

ABAQUS EXPERIMENTAL BAY MODEL

The finite-element simulation conducted in the study was carried out using Abaqus finite-element software. Abaqus is a widely used FE analysis tool to evaluate and predict the subsequent long-term behavior of concrete bridges. The objective of the FE analysis is the development of a model that predicts the stress-strain behavior of a bridge resulting from concrete shrinkage.

To study the effects of shrinkage as well as to better replicate full-scale bridges, large-scale bridge prototypes measuring 7 ft × 10 ft with an 8 in. thick slab were created using Abaqus (Figure 43). As shown in Figure 44, FE modeling included the concrete deck, girders, perimeter C-channels, and inside reinforcement.

The reinforcement was idealized using two-node linear truss elements that consider only axial strain along the reinforcement length (T3D2 elements). The experimental deck, supporting girders, and perimeter channels were modeled with eight-node linear brick elements (C3D8R continuum solid elements). Each node had three translational degrees of freedom in the x, y, and z directions. The brick elements utilize reduced integration to limit the number of integration points and reduce the running time without an unreasonable sacrifice of accuracy (Abaqus, 2014).

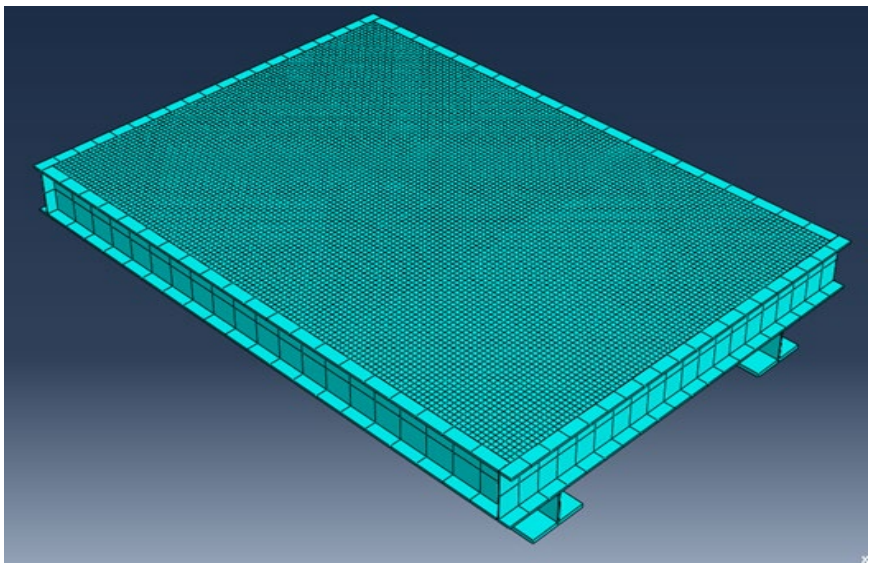

Figure 43. Illustration. Finite-element model of experimental deck.

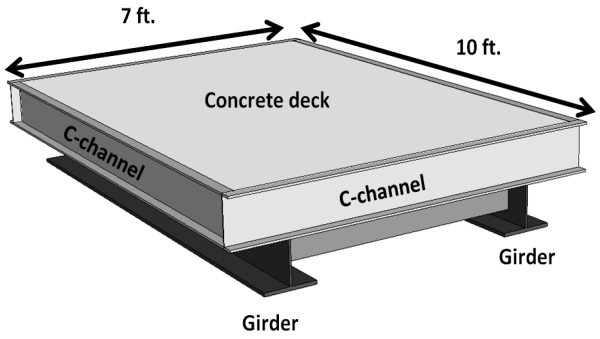

Figure 44. Illustration. Different parts of experimental deck.

Table 5 lists concrete and steel material properties used for FE modeling. A different elastic modulus and weight-per-unit volume were used for the different types of concrete according to the measured mixture properties. An elastic modulus value consistent with a 28-day unconfined compressive strength and a Poisson's ratio of 0.2 was selected for all concrete materials. The thermal coefficient of concrete usually varies between 3 to 8 × 10^{-6}/°F for normal-weight concrete (Abaqus, 2014). A thermal coefficient of 5.5 × 10^{-6}/°F was used for all types of concrete in this study.

Table 5. Material Properties Used in FE Models

	Control Concrete	Type K Concrete	LWA Concrete	SRA Concrete	Type K + LWA (I) Concrete	Type K + LWA (II) Concrete	Type K + Gypsum Concrete	Steel
Weight per unit volume (lb/ft^3)	142	141	136	142	135	139	142	490
Modulus of elasticity (ksi)	3770	3668	4380	4430	3878	4134	3798	29000
Poisson's ratio	0.2	0.2	0.2	0.2	0.2	0.2	0.2	0.3
Thermal coefficient of expansion (10^{-6}/°F)	5.5	5.5	5.5	5.5	5.5	5.5	5.5	6.5

Full bond was assumed between the steel and the concrete by sharing nodes at their intersection points. All elements in the large-scale model were bound by applying tied constraints, except for the reinforcement that was embedded inside the concrete deck, which allowed the concrete and reinforcement to act together when the concrete is expanding or shrinking.

EXPERIMENTAL DECK FINITE-ELEMENT RESULTS

Strains measured in the longitudinal reinforcement were chosen to be the primary focus for this research because they represent the mechanism by which transverse cracking is initiated in actual bridge decks. Concrete initially expands during the curing period followed by shrinkage upon

initiation of drying. Strain data were recorded for six months, and a negative strain indicates shrinkage.

It was not possible to model the drying shrinkage strain directly using the FE method in Abaqus and, as a result, an equivalent temperature load was used to model the shrinkage behavior of the concrete. More details are shown in Ardeshirilajimi et al. (2016). The average longitudinal total shrinkage strain (shown in Figure 41) was used to determine the equivalent temperature load.

The temperature load was calculated using the equation $\varepsilon = \alpha \Delta T$ and was uniformly applied within the deck. Here, ε represents the average longitudinal shrinkage strain collected from the experimental data, and α represents the thermal coefficient of expansion of concrete ($\alpha = 0.5 \times 10^{-6}$/°F). The strain ($\varepsilon$) divided by the thermal coefficient (α) yields the equivalent temperature load (ΔT). Figure 45 shows the temperature load applied to each type of concrete.

The developed FE models were verified using experimental results from the large-scale bridge decks previously described. These temperature loads permit shrinkage strains to be mimicked using Abaqus. The results from the comparison between the FE models and the experimental data are shown in Figures 46 through 52.

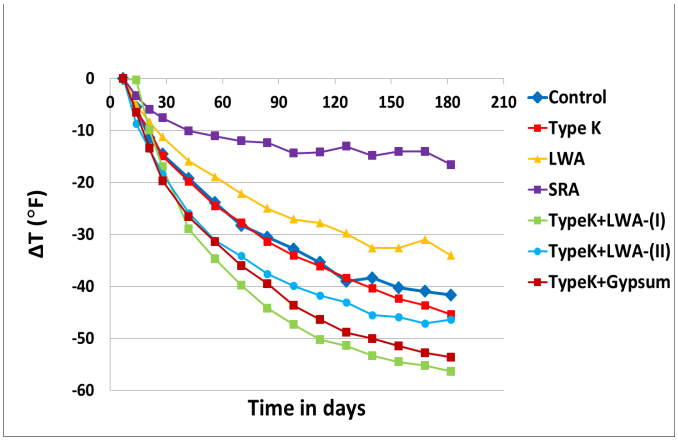

Figure 45. Graph. Temperature load applied to the FE model.

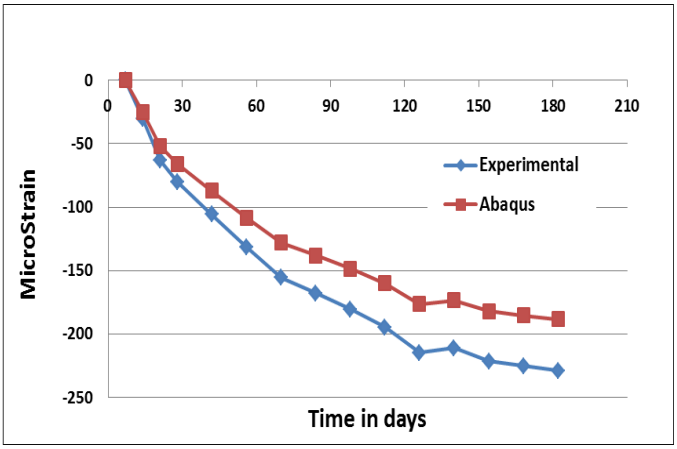

Figure 46. Graph. Control concrete deck (Ardeshirilajimi et al., 2016).

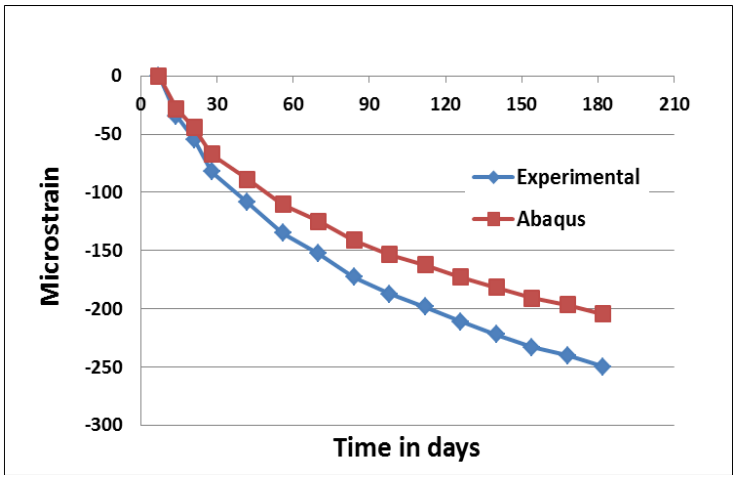

Figure 47. Graph. Type K concrete (Ardeshirilajimi et al., 2016).

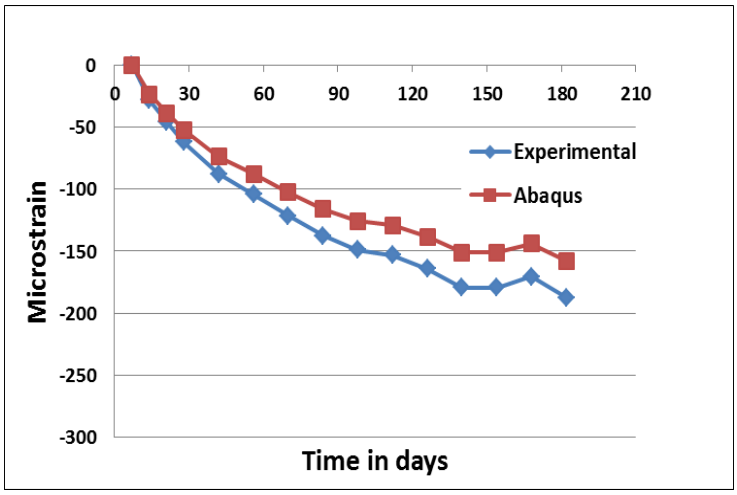

Figure 48. Graph. LWA concrete deck (Ardeshirilajimi et al., 2016).

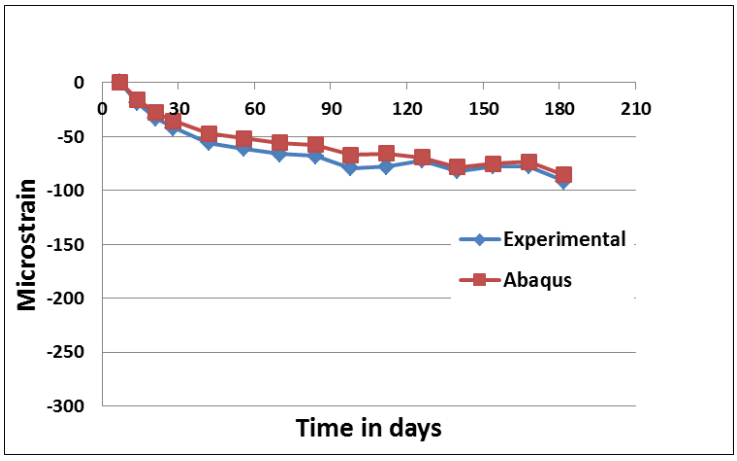

Figure 49. Graph. SRA concrete deck (Ardeshirilajimi et al., 2016).

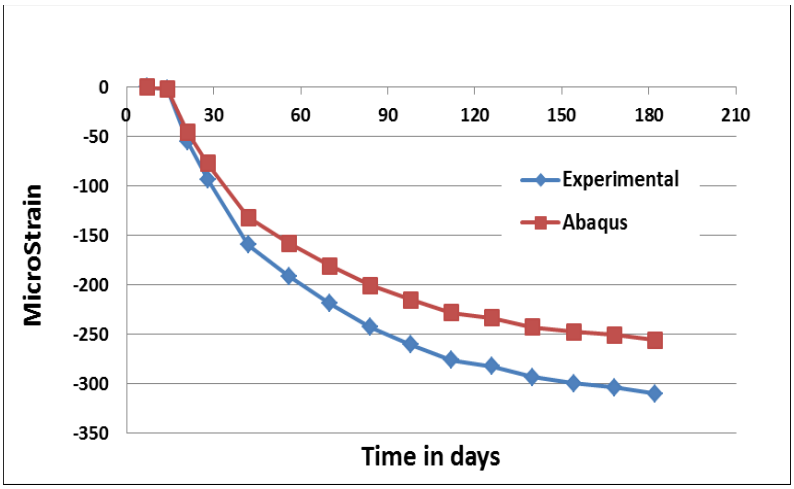

Figure 50. Graph. Type K+LWA (I) concrete deck.

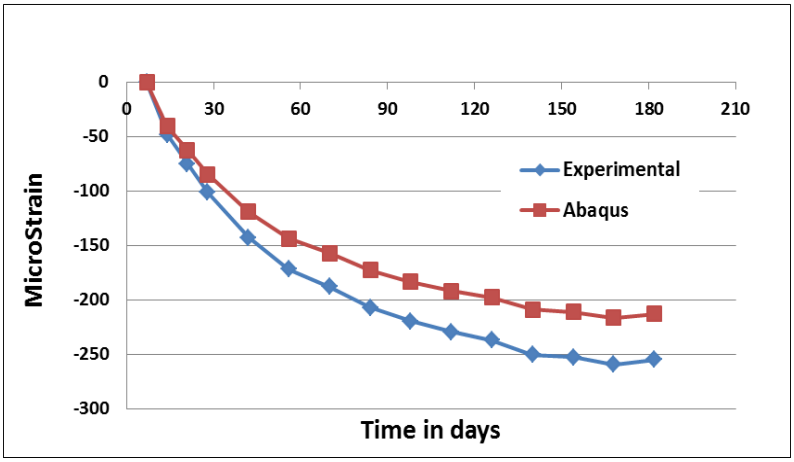

Figure 51. Graph. Type K+LWA (II) concrete deck.

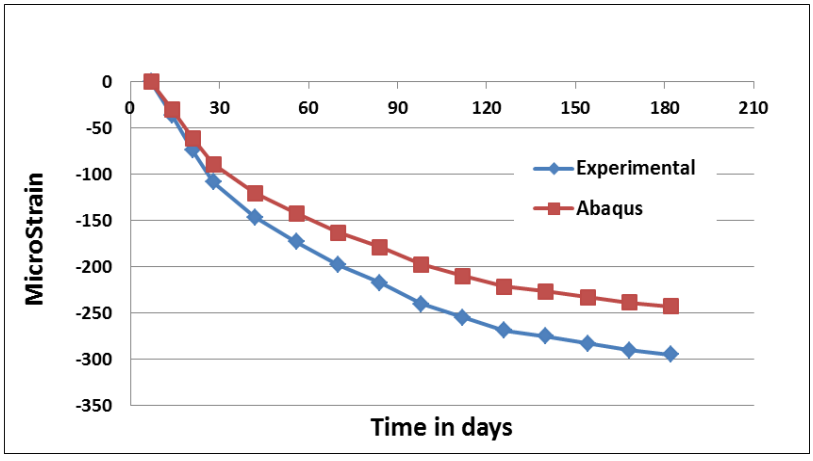

Figure 52. Graph. Type K+Gypsum concrete deck.

EXPERIMENTAL DECK PARAMETRIC STUDY

The finite-element model was used to monitor the stress and strain change within the concrete deck to predict the potential of cracking. One of the main objectives of this research was to carry an accurate parametric study of various factors that affect internal strain and stresses in a typical reinforced concrete bridge deck. A parametric study has been carried out to identify the effects of structural composition on concrete crack formation. This parametric study was done by altering the structure of the experimental deck using Abaqus in order to understand the variation of stresses due to shrinkage of the concrete when the structure is modified. The control deck model was used as the baseline for this part of the research; all material properties, boundary conditions, element types, and mesh size are the same as the control experimental deck.

The parametric study using the developed FE models was conducted using six structural parameters. The reinforcement bar size, rebar spacing, girder spacing, girder top flange width, concrete deck thickness, and girder support condition are the preliminary parameters considered for the parametric study. The minimum and maximum ranges of the selected parameters were considered carefully by following AASHTO LRFD standard and *Illinois Bridge Manual* specifications (AASHTO, 2014; IDOT, 2012). According to the *Illinois Bridge Manual* (IDOT, 2012) and AASHTO LRFD standard (AASHTO, 2014), the minimum and maximum size bar permitted in the bridge deck are #4 and #6, respectively.

The spacing between reinforcement bars is correlated with permitted reinforcement amount (As) inside the concrete deck. The minimum and maximum reinforcement amount (As) is 0.11 in^2/ft and 0.6 in^2/ft, respectively, in each layer of reinforcement (AASHTO, 2014). In this parametric study, spacing between reinforcement bars was selected between 4 in. to 18 in.

The spacing between girders varies from 3.5 ft to 12 ft, as recommended in the *Illinois Bridge Manual* (IDOT, 2012). In the parametric study, spacing between girders were selected as 5 ft and 6 ft by considering the size of the bridge deck.

The experimental deck was supported by two W 12×79 steel girders with a top flange width of 12 in. In the parametric study, another girder (W10×77) was selected by considering a similar cross-sectional area with a top flange width of 10 in. Two different top flange widths were considered to investigate the effect on concrete shrinkage.

The thickness of the bridge deck preliminarily selected was based on the spacing between two girders. The minimum permitted bridge thickness is 7 in. by AASHTO standards. The *Illinois Bridge Manual* (IDOT, 2012) recommends a deck thickness of 8 in. for girder spacing between 5 ft to 9.5 ft. In the parametric study, concrete deck thickness was selected as 7 in. and 8 in. by considering the spacing between girders. Two different support conditions were chosen as simply supported (pinned-roller) and fixed-fixed at the bottom end of the girders.

The parametric study was performed in three steps by considering all selected parameters. The first two parameters were correlated with each other, as changing the rebar size and spacing also changes the reinforcement amount inside the concrete deck.

In the first step, six FE model cases were developed considering rebar size, spacing, and reinforcement, as shown in Tables 6 and 7. The first six FE model cases were developed after considering the same amount of reinforcement (As) by changing rebar size and spacing. When the rebar size was changed, rebar spacing must be changed accordingly in order to maintain the same amount of reinforcement inside the concrete deck.

Table 6. List of FE Model Performed—Top Layer Reinforcement Size and Spacing

FE Model	Rebar Size	Rebar Spacing, in.	Top Layer Reinforcement Amount (As), in^2
Case 1	#4	8	**2.2**
Case 2 (original)	#5	12	**2.17**
Case 3	#6	18	**2.2**

Table 7. List of FE Model Performed—Bottom Layer Reinforcement Size and Spacing

FE Model	Rebar Size	Rebar Spacing, in.	Bottom Layer Reinforcement Amount (As), in^2
Case 4	#4	4	**2.2**
Case 5 (original)	#5	8	**2.17**
Case 6	#6	10	**2.2**

Figures 53 through 56 show the strain and stress on the top and bottom layers of reinforcement, respectively, based on the FE model developed in Tables 6 and 7. The results from the first six FE models showed that changing the rebar size and spacing did not significantly change the average strain (Figures 53 and 54) and stress (Figures 55 and 56) in the longitudinal direction at the end of the six-month period. The internal strain and stress showed an insignificant change as the reinforcement amount remains the same for all cases.

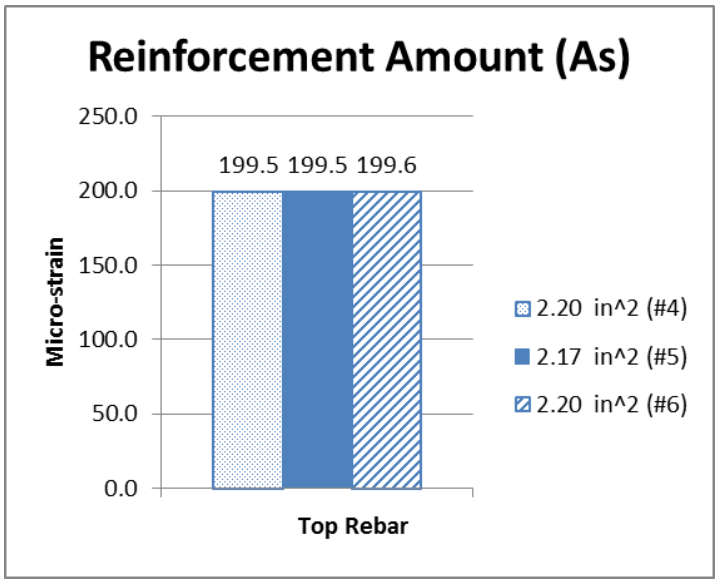

Figure 53. Chart. Strain at 182 days on the top layer.

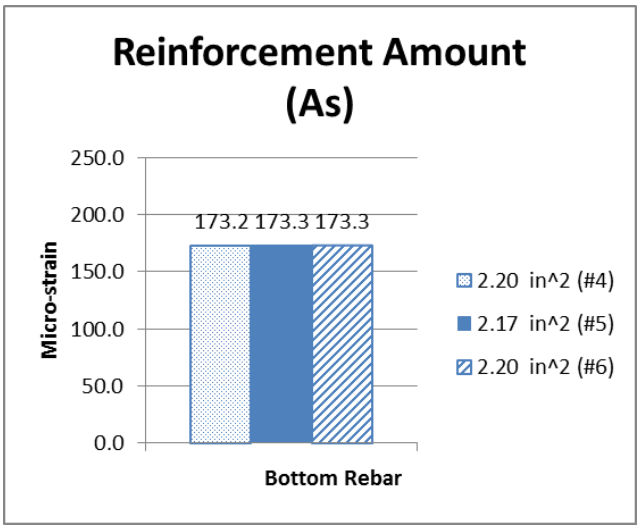

Figure 54. Chart. Strain at 182 days on the bottom layer.

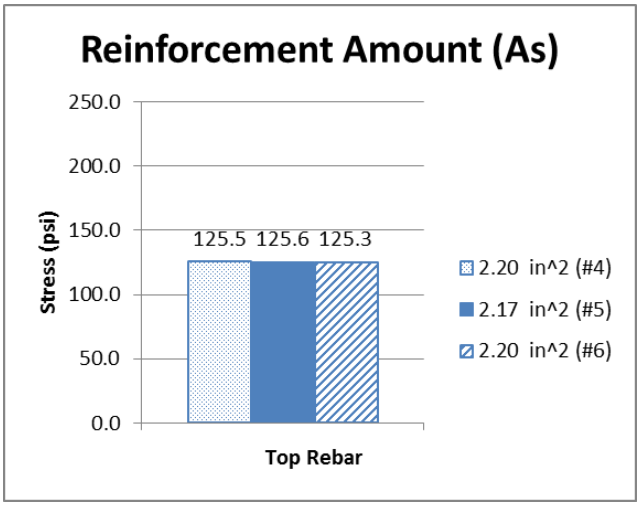

Figure 55. Chart. Stress at 182 days on the top layer.

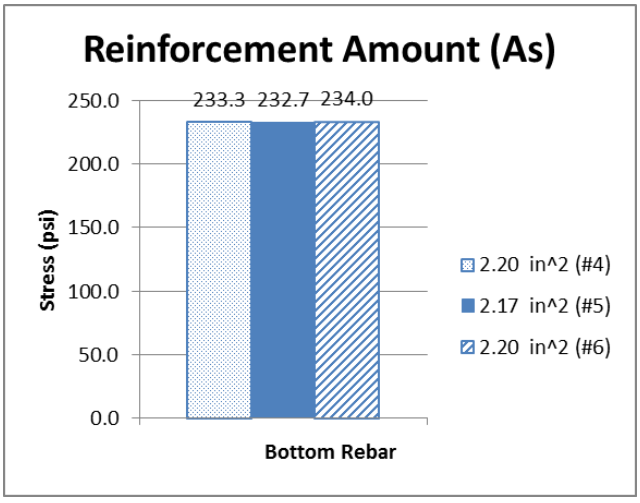

Figure 56. Chart. Stress at 182 days on the bottom layer.

In the second step, three FE model cases were developed after considering the same rebar spacing by changing the rebar size and spacing, as shown in Table 8. In these three model cases, rebar size and reinforcement amount (As) must be changed accordingly to maintain the same rebar spacing in the concrete deck. The total amount of reinforcement varied between 3.00 in^2 to 6.60 in^2 (Table 8).

Table 8. List of FE Model Performed—Considering Same Rebar Spacing

	Top Layer			Bottom Layer			Total As
FE Model	**Rebar Size**	**Rebar Spacing, in**	**Reinforcement Amount (As), in^2**	**Rebar Size**	**Rebar Spacing, in**	**Reinforcement Amount (As), in^2**	
Case 7	#4	12	**1.40**	#4	8	**1.60**	**3.00**
Case 8	#5	12	**2.17**	#5	8	**2.48**	**4.65**
Case 9	#6	12	**3.08**	#6	8	**3.52**	**6.60**

Figures 57 through 60 show the strain and stress on the top and bottom layers of reinforcement, respectively, based on the FE model developed in Table 8. The results from the FE model as shown in Table 8 show that changing the rebar size and reinforcement amount changes the average strain in the longitudinal direction at the end of a six-month period (Figures 57 and 58). The results inside the concrete deck also show a significant stress change as the reinforcement amount changes (Figures 59 and 60). The results indicate higher stresses are induced when a higher level of restraint or reinforcement amount was presented inside the concrete deck.

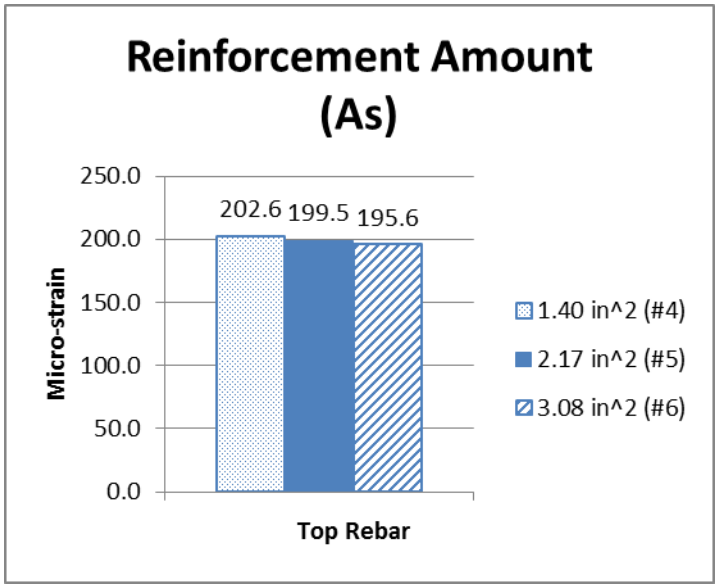

Figure 57. Chart. Strain at 182 days on the top layer.

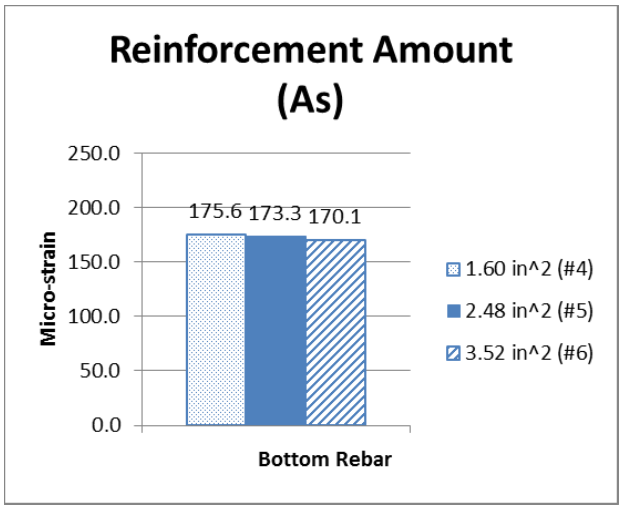

Figure 58. Chart. Strain at 182 days on the bottom layer.

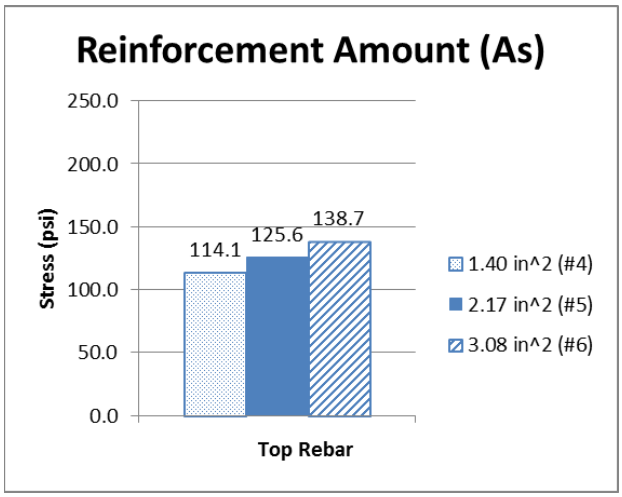

Figure 59. Chart. Stress at 182 days on the top layer.

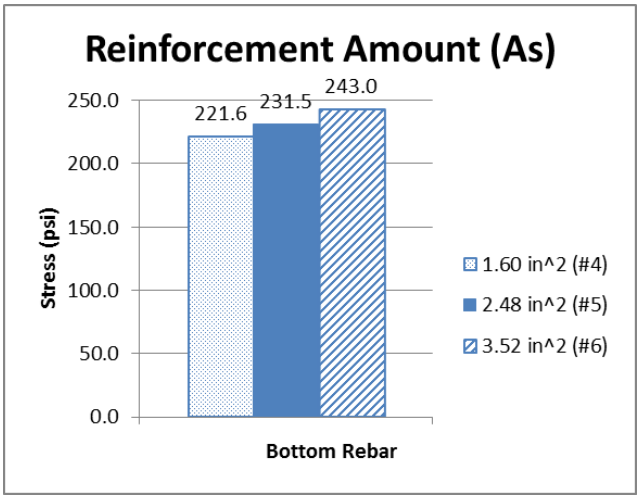

Figure 60. Chart. Stress at 182 days on the bottom layer.

Design of Experiment Method

In this section, various parameters were investigated by following the design of experiment (DOE) method. In the DOE method, parameters varied simultaneously and the interactions between those parameters were investigated. The 2^n full factorial assumes a linear trend between the parameters by considering low- and high-bound values for each parameter. The reinforcement amount showed a significant effect on concrete shrinkage after considering rebar size and spacing from the second step of the parametric study. Therefore, in the third step of the parametric study, five preliminary parameters were selected to study the structural effect on concrete shrinkage, as listed in Table 9. In this step, the reinforcement amount was chosen from the total amount of reinforcement presented in Table 8, which varies between 3.00 in^2 to 6.60 in^2. The low- and high-bound range of the parameters were selected carefully by considering possible minimum and maximum values by following AASHTO LRFD standard and *Illinois Bridge Manual* specifications (AASHTO 2014; IDOT, 2012).

Table 9. Parameters in DOE Model

Parameter	Label	Low Value (−1)	High Value (1)
Reinforcement amount	A	3 in^2	6.6 in^2
Girder spacing	B	5 ft	6 ft
Flange width	C	10 in.	12 in.
Deck thickness	D	7 in.	8 in.
Support condition	E	Pin-Roller	Fix-Fix

Based on the DOE method, multiple cases (runs) were investigated to develop an analysis matrix that simultaneously examines the individual and interactive effects of each considered parameter. Table 10 shows 32 cases (n = 5 parameters, where $2^n = 32$) considered in this parametric study to assemble the matrix for the DOE analysis.

The “main-effect” plot presents the mean values for low and high ranges of each parameter, and both values were connected by a straight line. In the DOE main-effect graph when the connected line is not horizontal, the response (concrete shrinkage) changes between the low- and high-bound range for that individual parameter. A higher slope of the line indicates a larger effect of parameters in the response or shrinkage. In contrast, a horizontal connected line between the low- and high-bound range illustrates no effect of that individual parameter. A horizontal line shows the same response across all levels between the ranges.

Figure 61 (A-E) shows the DOE main-effect plot of the five considered parameters. The main-effect plot for the reinforcement amount (Figure 61-A) showed a sloped line. In Figure 61-A, the #6 rebar results more strain value compared to the #4 reinforcement bar. More restraint from the #6 rebar results in a higher concrete shrinkage strain value of 216 με (absolute value for better understanding) compared with less shrinkage strain (213 με) from the #4 reinforcement bar. A similar trend and effect are observed for the flange width, deck thickness, and support condition parameters (Figure 61-C to E).

Figure 61-B shows the DOE main effect of the girder spacing. The smaller girder spacing (5 ft) created larger concrete strain within the deck when compared with larger spacing (6 ft). In other words, compared to larger girder spacing (6 ft), smaller spacing (5 ft) between girder caused larger shrinkage strain due to higher structural restraint.

Table 10. Parameter Matrix in DOE Model

Case (run)	A	B	C	D	E
1	−1	−1	−1	−1	−1
2	1	−1	−1	−1	−1
3	−1	1	−1	−1	−1
4	1	1	−1	−1	−1
5	−1	−1	1	−1	−1
6	1	−1	1	−1	−1
7	−1	1	1	−1	−1
8	1	1	1	−1	−1
9	−1	−1	−1	1	−1
10	1	−1	−1	1	−1
11	−1	1	−1	1	−1
12	1	1	−1	1	−1
13	−1	−1	1	1	−1
14	1	−1	1	1	−1
15	−1	1	1	1	−1
16	1	1	1	1	−1
17	−1	−1	−1	−1	1
18	1	−1	−1	−1	1
19	−1	1	−1	−1	1
20	1	1	−1	−1	1
21	−1	−1	1	−1	1
22	1	−1	1	−1	1
23	−1	1	1	−1	1
24	1	1	1	−1	1
25	−1	−1	−1	1	1
26	1	−1	−1	1	1
27	−1	1	−1	1	1
28	1	1	−1	1	1
29	−1	−1	1	1	1
30	1	−1	1	1	1
31	−1	1	1	1	1
32	1	1	1	1	1

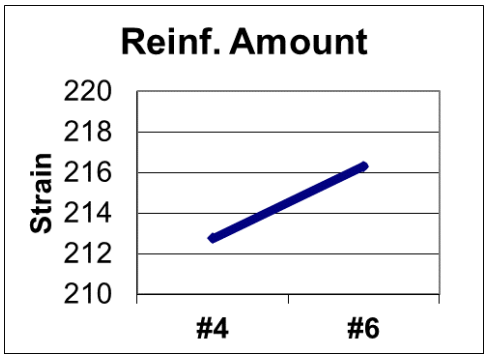
Reinf. Amount
Strain
220
218
216
214
212
210
#4
#6

(a)

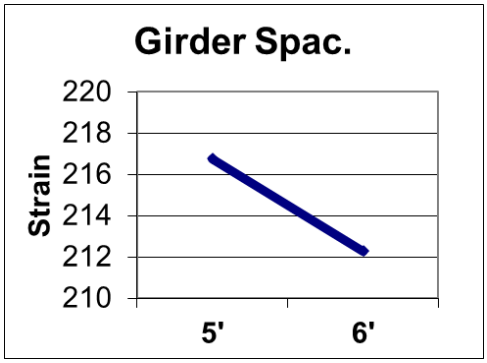
Girder Spac.
Strain
220
218
216
214
212
210
5'
6'

(b)

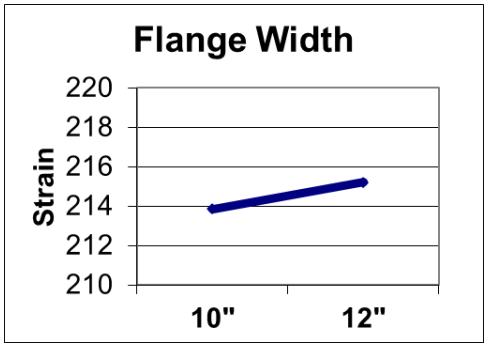
Flange Width
Strain
220
218
216
214
212
210
10"
12"

(c)

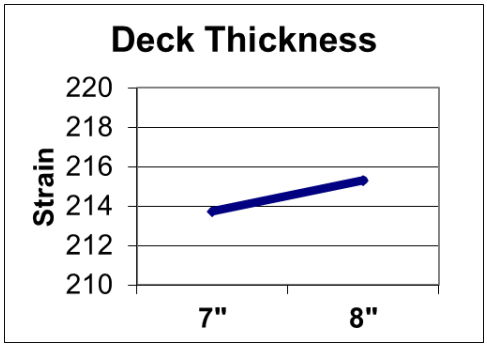
Deck Thickness
Strain
220
218
216
214
212
210
7"
8"

(d)

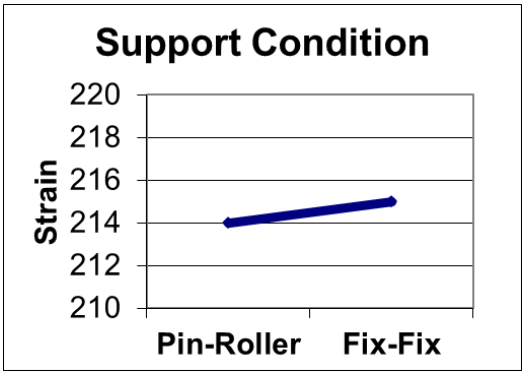

(e)

Figure 61. Graph. DOE main effect of each parameter on concrete strain.

Figure 62 shows the results from the DOE main-effect plot for the selected parameters. The results indicate higher stresses were induced when a higher level of restraint was presented. The resultant DOE plot illustrates that increasing the amount of reinforcement inside the bridge deck significantly increases the stress in the concrete (Figure 62-A). Flange top width and support condition showed a similar effect as reinforcement amount (Figure 62-C and Figure 62-E). However, Figure 62-B shows that the smaller girder spacing (5 ft) created larger average stress within the deck when compared with larger spacing (6 ft).

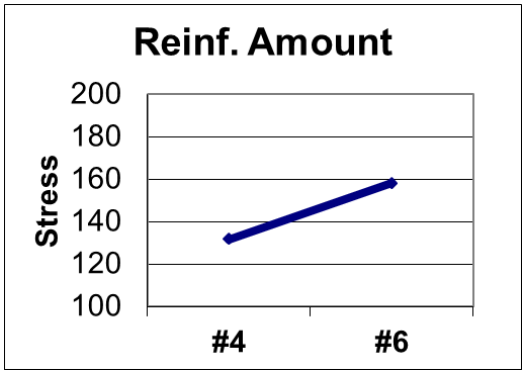

(a)

(b)

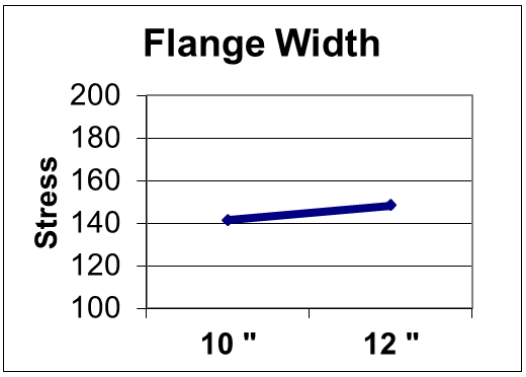

(c)

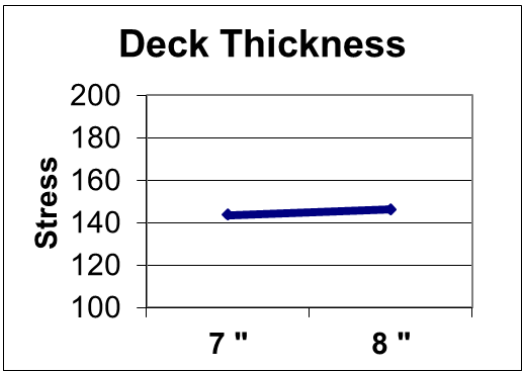

(d)

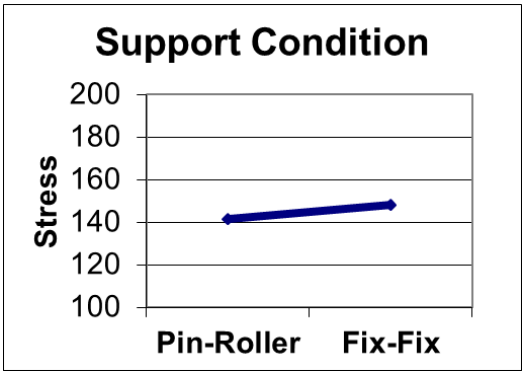

(e)

Figure 62. Graph. DOE main effect of each parameter on concrete stress.

Cracking in bridge decks occurs when concrete tries to change its volume but is restrained from movement. More structural restraint limits the concrete from volumetric change. More restraint from the surrounding structural element causes higher tensile stress in concrete. In other words, more restraint from the structural element allows less volumetric changes in concrete, which results in more tensile stress in the concrete due to higher restraint.

SUMMARY

Finite-element modeling for the experimental deck was conducted by applying temperature load to the concrete to predict shrinkage. Different concrete mixtures were modelled with Abaqus, which was able to predict the shrinkage strain inside the deck with minimal difference at the end of six months. A parametric study using DOE analysis shows that higher restraint from surrounding structural element leads to higher tensile stress. More restraint from internal reinforcement, less girder spacing, larger girder flange width, and more restrictive support conditions increase the concrete tensile stress and lead to potential cracking in the concrete deck.

CHAPTER 4: CONCLUSIONS

The main conclusions of this study are as follows:

- The experimental deck poured with SRA showed the least amount of shrinkage compared with other mitigating mixtures.
- The Type K mixture showed higher early-age expansion compared with the control mixture.
- During the drying period, internally cured LWA slowly released the absorbed water, which resulted in a slower shrinkage rate.
- The combination of Type K and internally cured LWA mixtures showed the highest peak strain during the hydration period.
- The combined mixture of Type K expansive cement and gypsum mineral did not show any notable strain difference compared with the individual Type K mixture when investigated in a large-scale experimental deck.
- In comparing the total shrinkage strain following the initial expansion, the experimental deck containing the Type K+LWA (I) mixture had the largest total shrinkage compared with all mitigating mixtures.
- Quality control to accurately measure the amount of water added in the combined mixture of Type K cement and internally cured LWA is important.
- Strain values from concrete gauges were almost identical with the strain values of reinforcement (foil gauges), indicating that the concrete and reinforcement were fully bonded.
- Temperature load applied in the finite-element simulation was used to predict the shrinkage of concrete decks with reasonable accuracy.
- The stress and strain inside the concrete deck showed insignificant change with a similar amount of reinforcement by changing different reinforcement size and spacing.
- The parametric study showed that a higher amount of internal restraint in the deck produced higher tensile stress within the deck.

REFERENCES

American Association of State Highway and Transportation Officials (AASHTO). (2014). *LRFD bridge design specifications*. AASHTO.

Abaqus. (2014). *Abaqus 6.14 analysis user's manual*. Abaqus.

Aimin, X., & Sarkar, S. L. (1991). Microstructural study of gypsum activated fly ash hydration in cement paste. *Cement and Concrete Research, 21*(6), 1137–1147. https://doi.org/10.1016/0008-8846(91)90074-R

Ardeshirilajimi, A., Wu, D., Chaunsali, P., Mondal, P., Chen, Y. T., Rahman, M. M., et al. (2016). *Bridge decks: Mitigation of cracking and increased durability* (Report No. FHWA-ICT-16-016). Illinois Center for Transportation.

American Society for Testing and Materials (ASTM C39). (2014). *Standard Test Method for Compressive Strength of Cylindrical Concrete Specimens*.

Arezoumandi, M. (2015). *Feasibility of crack free reinforced concrete bridge deck from materials composition perspective: a state of the art review*. Frontiers of Structural and Civil Engineering, 9(1), 91-103.

Bentz, D. P., & Weiss, W. J. (2011). *Internal curing: A 2010 state-of-the-art review*. US Department of Commerce, National Institute of Standards and Technology.

Chaunsali, P., Lim, S., Mondal, P., Foutch, D. A., Richardson, D., Tung, Y., & Hindi, R. (2013). *Bridge decks: Mitigation of cracking and increased durability* (Report No. FHWA-ICT-13-023). Illinois Center for Transportation.

French, C., Eppers, L., Le, Q., & Hajjar, J. (1999). *Transverse cracking in concrete bridge decks* (Report No. MN/RC-1999-05). University of Minnesota.

Frosch, R. J., Blackman, D. T., & Radabaugh, R. D. (2002). *Investigation of bridge deck cracking in various bridge superstructure systems* (Report No. FHWA/IN/JTRP-2002/25). Joint Transportation Research Program. https://doi.org/10.5703/1288284313257

Hadidi, R., & Saadeghvaziri, M. A. (2005). *Transverse cracking of concrete bridge decks: state-of-the-art*. Journal of Bridge Engineering, 10(5), 503-510.

Illinois Department of Transportation (IDOT). (2012). *Bridge manual*. Illinois Department of Transportation.

Nagataki, S., & Gomi, H. (1998). Expansive admixtures (mainly ettringite). *Cement and Concrete Composites, 20*(2), 163–170. https://doi.org/10.1016/S0958-9465(97)00064-4

Pittman, D. W., Ramey, G. E., Webster, G., & Carden, A. (1999). Laboratory evaluation of concrete mixture designs employing type I and type K cement. *Journal of Materials in Civil Engineering*, *11*(2), 144–150. https://doi.org/10.1061/(ASCE)0899-1561(1999)11:2(144)

Rahman, M., Chen, Y., Ibrahim, A., Lindquist, W., Tobias, D., Krstulovich, J., et al. (2020). Study of drying shrinkage mitigating concrete using scaled bridge bays. *International Journal of Civil Engineering, 18*(1), 65–73. https://doi.org/10.1007/s40999-019-00460-z

Rahman, M., Chen, Y., Lindquist, W., Ibrahim, A., & Hindi, R. (2018). *Mitigation of shrinkage cracking in bridge decks using Type-K cement.* Paper presented at the Structural Congress 2018, Fort Worth, Texas, April 19–21. https://doi.org/10.1061/9780784481332.011

Rahman, M., Chen, Y., Lindquist, W., Ibrahim, A., Tobias, D., Krstulovich, J., & Hindi, R. (2019). Large-scale testing of shrinkage mitigating concrete. *Journal of Sustainable Cement-Based Materials, 8*(1), 39–54. https://doi.org/10.1080/21650373.2018.1514671

Rahman, M., Gonzalez, D., & Hindi, R. (2019). *Combined effect of expansive cement and internal curing to mitigate shrinkage cracking in bridge decks.* Paper presented at the Structures Congress 2019, Orlando, Florida, April 24–27. https://doi.org/10.1061/9780784482230.006

Richardson, D., Tung, Y., Tobias, D., & Hindi, R. (2014). An experimental study of bridge deck cracking using type K-cement. *Construction and Building Materials, 52*(1), 366–374. https://doi.org/10.1016/j.conbuildmat.2013.11.052

Schmitt, T. R., & Darwin, D. (1995). *Cracking in concrete bridge decks*. University of Kansas Center for Research, Inc.

Tej, P., Čech, J., Kolísko, J., Čítek, D., & Vítek, J. L. (2014). Experimental measurements and computer analysis of heat of hydration and shrinkage of large-scale model of reinforced concrete slab. *Advanced Materials Research*, *1004–1005*, 1594–1597. https://doi.org/10.4028/www.scientific.net/amr.1004-1005.1594

APPENDIX: LARGE-SCALE TESTING RESULTS

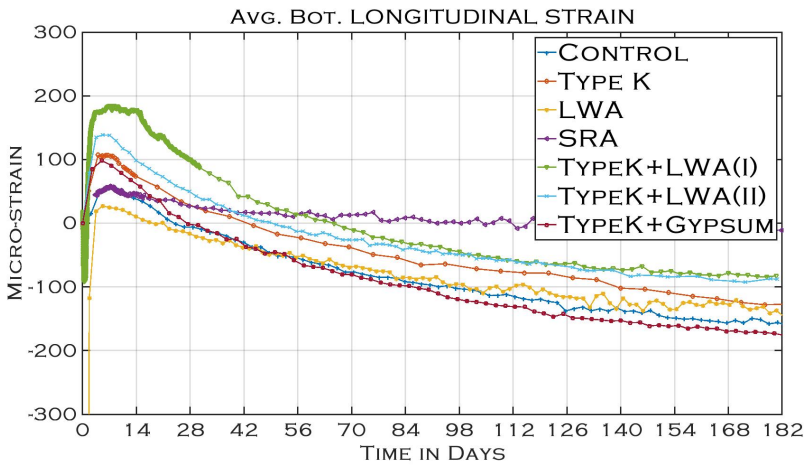

Figure 63. Graph. Average top transverse strain.

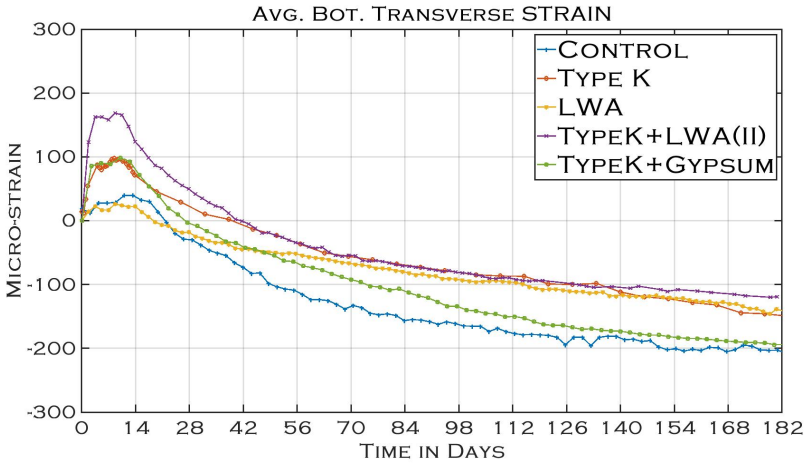

Figure 64. Graph. Average bottom transverse strain.


Illinois Department
of Transportation


ILLINOIS